Silver Nanowire Transparent Electrodes: Fabrication, Characterization, and Device Integration

by

Hadi Hosseinzadeh Khaligh

A thesis

presented to the University of Waterloo

in fulfillment of the

thesis requirement for the degree of

Master of Applied Science

in

Electrical and Computer Engineering -Nanotechnology

Waterloo, Ontario, Canada, 2013

AUTHOR'S DECLARATION

I hereby declare that I am the sole author of this thesis. This is a true copy of the thesis, including any required final revisions, as accepted by my examiners.

I understand that my thesis may be made electronically available to the public.

Abstract

Silver nanowire transparent electrodes have recently received much attention as a replacement for indium tin oxide (ITO) for use in various electronic devices such as touch panels, organic solar cells, and displays. The fabrication of silver nanowire electrodes on glass substrates with a sheet resistance as low as 9 Ω/□ and 90% optical transparency at 550 nm is demonstrated. These resistance and transparency values match that of commercially available indium tin oxide and are superior to other alternatives such as carbon nanotube electrodes. The nanowire electrodes are low cost and easy to fabricate. Moreover, by depositing nanowire films on plastic substrates, mechanically flexible electrodes are obtained. The silver nanowire electrodes are integrated into several electronic devices: transparent heaters, organic solar cells, and switchable privacy glass.

The concerns about the suitability of silver nanowire electrodes for use in commercial electronic devices are discussed. High surface roughness, one of the major concerns, is addressed by introducing a new method of embedding silver nanowires in a soft polymer. The instability of silver nanowire electrodes under current flow is also demonstrated for the first time. It is shown that silver nanowire electrodes fail under current flow after as little as 2 days. This failure is caused by Joule heating which causes the nanowires to break up and thus create an electrical discontinuity in the nanowire film. Suggestions for improving the longevity of the electrodes are given.

Acknowledgements

I would like to thank Professor Irene Goldthorpe for all of her support, encouragement, and guidance as my supervisor.

I am also thankful to my wife, for all her support, and patience.

Special thanks to my parents, who have been patient to my absence, what I have achieved in my life belong to them.

Dedication

This thesis is dedicated to my parents and my wife who will be happy to see my graduation.

Contents

List of Figures

Chapter 1

Introduction

1.1. Transparent electrodes

Transparent electrodes are a crucial part of many electronic devices such as organic solar cells, displays (e.g. Liquid Crystal Displays (LCDs)), touch panels, and transparent heaters. Transparent electrode thin films are optically transparent to visible light and also electrically conductive, and are used in applications where light needs to enter or leave a device. For instance, in organic solar cells a transparent electrode acts as either an anode or cathode and completes the solar cell circuit while at the same time lets visible light pass through the film to generate charge carriers [1]. Figure 1.1a shows a schematic of an organic solar cell. In this structure, indium tin oxide (ITO), which is a transparent conductive film deposited on a glass substrate, is used as the anode of the device.

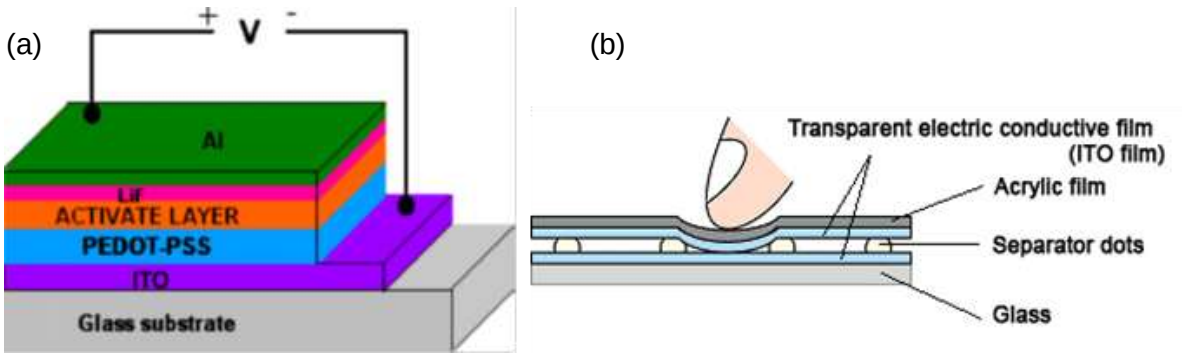

Figure 1.1 (a) Structure of basic unit of an organic solar cell [1]. (b) Structure of a resistive touch panel [2].

Transparent electrodes are also used in touch panels, as illustrated in Figure 1.1b [2]. This device consists of two layers of transparent electrodes. Also on the market are transparent heaters, made of transparent electrodes and used to remove frost from displays, cameras and also ski goggles in cold environments. Figure 1.2 shows a commercial example of an ITO transparent heater [3].

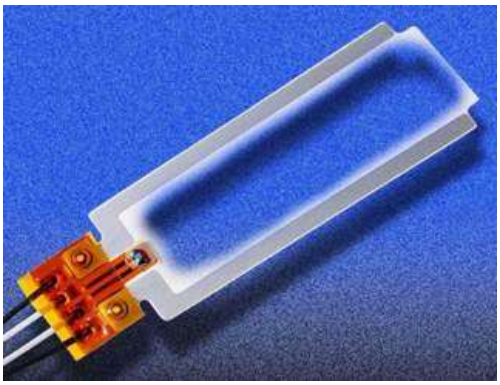

Figure 1.2 An ITO transparent heater being used as a defroster [3].

The most common materials used for transparent electrodes are metal oxides, particularly ITO which is the most popular material for transparent electrodes. ITO can provide highly transparent electrodes (80-95%) with low sheet resistances (10-1000 Ω/□).

Metal oxides are transparent because their band gap energies are larger than the energies of photons in the visible range. The band gap of ITO, for example, is 3.8 eV [4]. Figure 1.3 shows the optical spectra of ITO, which is typical for metal oxide transparent electrodes. The sample with a sheet resistance of 10.98 Ω/□ in the figure is about 80% transparent at wavelengths between 400 and 700 nm; in this region, film interference effects can be seen in both the transmission and reflection spectra. High absorption below 300 nm wavelengths is due to the band gap of the material. Above 1000 nm, transmittance decreases drastically which corresponds to collective oscillations of conduction band electrons, known as plasma oscillations or plasmons [4].

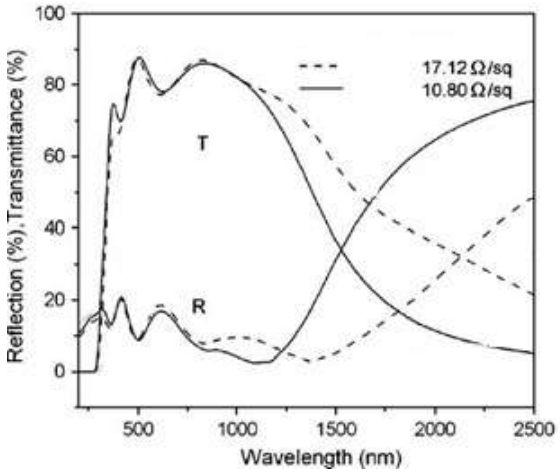

Figure 1.3 Optical spectra of typical ITO transparent conductors including both reflection (R) and transmittance (T) [5].

For a particular application, the transparency and sheet resistance of an ITO film can be controlled through the film thickness [4]. Figure 1.4 shows that there is a trade-off between transparency and resistance; lower resistivity films require a thicker ITO layer, which results in lower transparency.

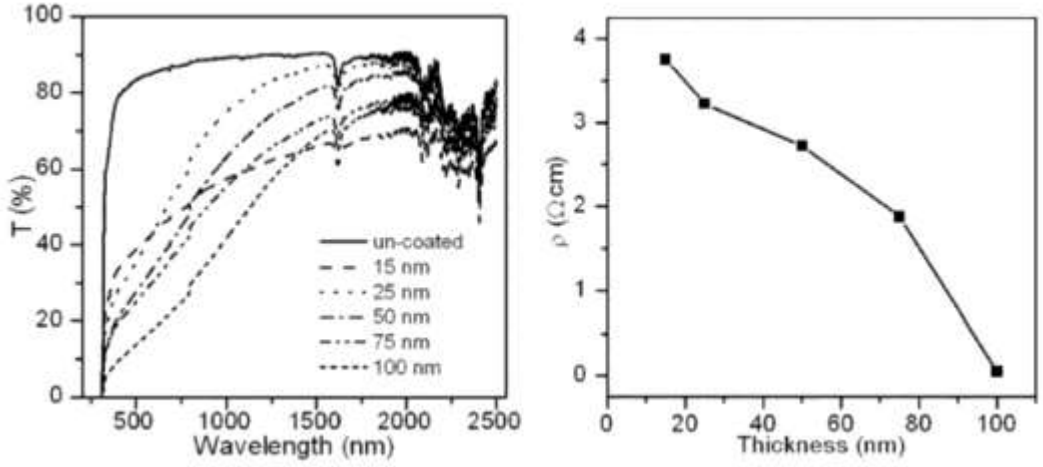

Figure 1.4 Transmittance of ITO for different thicknesses (left). ITO film resistivity changes depending on its thickness (right) [6].

In the last decade, the number of electronic displays and touch screens has increased drastically. For example, 362 million touch panels were produced in 2010 with an increase of 20% each year up to 2013 [7]. In addition, new device technologies call for new features for transparent electrodes like flexibility, easy fabrication processes, low cost and light weight.

ITO cannot meet all the new expected qualifications for the innovative next generation of electronics. ITO has ceramic properties, so it is not flexible; a small amount of strain as low as 2-3% can initiate cracks in ITO film on flexible substrates, which reduces electrode conductivity and thus performance of the device dramatically [8]. Secondly, indium is a rare material and the price of indium is volatile with an overall increasing trend [9]. Thirdly, the fabrication of ITO is costly since it requires high temperatures and a high vacuum for control over the thickness and doping concentration [9] Also, it is deposited by sputtering which can damage underlying layers in the case of organic devices. Fourthly, ITO also has a high index of refraction, which is not suitable for display applications since it reflects light whereby decreasing the brightness of the screen. An additional coating needs to be applied to solve this problem, leading to additional cost.

Extensive research has been devoted to solving problems associated with ITO transparent electrodes. For example, to make a flexible ITO transparent electrode, ITO has been laminated onto flexible substrates like polyethylene terephthalate (PET), and ITO elements in various ratios have been investigated to improve the mechanical properties of the film [9]. However, these approaches not only add additional manufacturing cost but also reduce the optical and electrical performance of such electrodes so they cannot compete in the current growing market. Therefore, over the past decade many researchers have tried to find an alternative material to replace ITO. So far they have made significant advances in introducing new potential candidates

for transparent electrodes. However, each candidate has advantages and disadvantages and more investigation is need before any of them can be used commercially. Current significant materials for substitution are carbon nanotubes (CNTs), graphene, transparent conductive polymers, metal grids, and random meshes of metal nanowires.

1.2. Carbon nanotube electrodes

The first CNTs were synthesized in 1990 [10]. A single carbon nanotube can have electron mobilities higher than 100 000 $cm^2/V.s$ [11] and CNTs have also been shown to have unique and beneficial optical and mechanical properties [12-13]. Films of CNTs appeared in the mid-2000s as a new material for transparent electrodes as illustrated in Figure 1.5 [9]. Although it was thought they would be a suitable ITO substitute because of their high mobility, challenges emerged for CNT films.

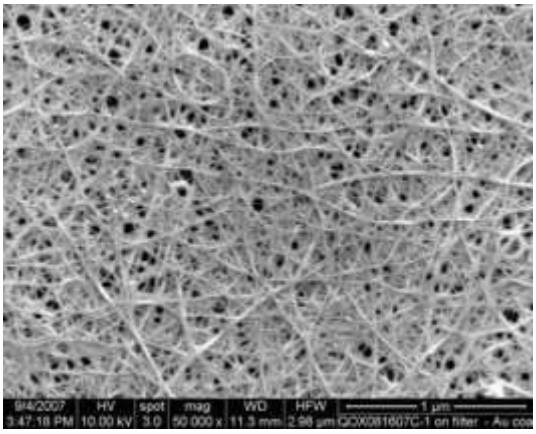

Figure 1.5 Single-wall carbon nanotube film [14]

The most important challenge relates to the conductivity of CNT films, which is limited by the junction resistance where nanotubes overlap. These junctions between nanotubes have high resistance in the range of 200 kΩ - 20 MΩ [11]; hence, the conductivity of CNT films is reduced drastically compared to that of a single CNT. Some approaches have been introduced to reduce the sheet resistance of the CNT films such as treating CNTs with acid and using longer CNTs

[9]. Figure 1.6 shows the sheet resistance vs. transmittance of a CNT film before and after acid treatment [15]. However, films of CNTs still have much lower conductivity than conventional ITO films. A related problem to the junction resistance is that CNTs can be either metallic or semiconducting. In CNT fabrication, semiconductor and metal CNT are fabricated at the same time so the CNT films consist of both types. The semiconductor nanotubes have much lower conductivity than the metallic tubes [11] and so do not contribute much to the conductivity. However, the semiconductor nanotubes absorb light and so reduce transparency. In addition, metal/semiconductor junctions in CNT films create high contact resistance due to Schottky barrier formation, resulting in higher sheet resistance [11]. Separating metal and semiconductor CNTs or producing metallic only CNT are still serious challenges. Although some methods have been introduced to separate metal nanotubes, they are expensive and not suitable for commercial use [6].

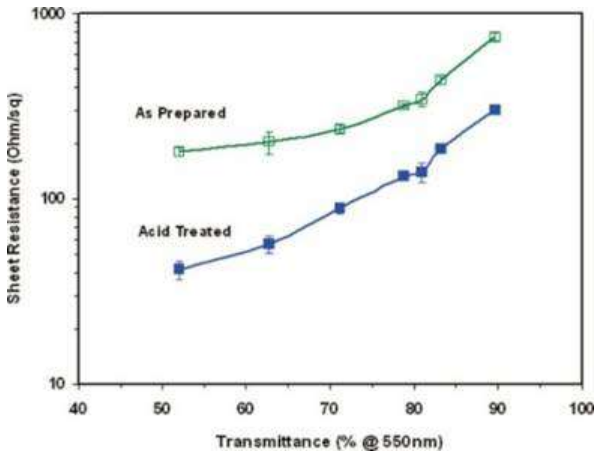

Figure 1.6 Sheet resistance versus transmittance for single-wall nanotubes (SWNT) films with varying thicknesses, before and after acid treatment [15]. Although the acid treatment reduces the resistance of the films by reducing the junction resistances, the overall sheet resistance of the films is still much higher than ITO.

The best results for CNT transparent electrodes are gathered in Figure 1.7 [16], and show a significant progress in fabricating transparent electrodes based on CNTs during recent years. However, most applications require lower sheet resistances and higher transparency than even

the best values shown in the plot and thus CNT films at this time are not a suitable replacement for ITO [17–25].

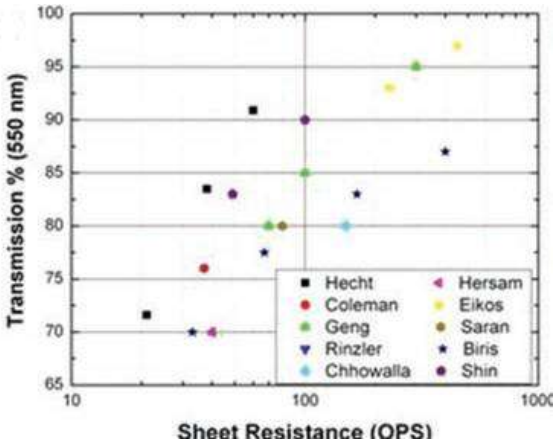

Figure 1.7 Sheet resistance vs. transmittance for the highest conductivity CNT films. References in plot [14-25].

1.3. Graphene electrodes

Graphene is a thin layer of carbon atoms bonded with sp2 orbitals. Among the interesting properties of graphene is the capability of adding external dopants which results in high in-plane conductivity of graphene sheets. The thickness of the graphene sheets is in the order of a few nanometers and thus, the graphene sheets are relatively transparent to visible light.

The major concern regarding graphene is that fabrication of a single sheet of graphene on a large scale is difficult. More often, instead of a single sheet of graphene, networks of graphene flakes are synthesized. These flakes result in very high sheet resistance, in the range of several kΩ [9], because there is a high contact resistance between flakes so the overall conductivity is low [26-27]. Figure 1.8 shows the boundaries and contact areas that cause high resistivity.

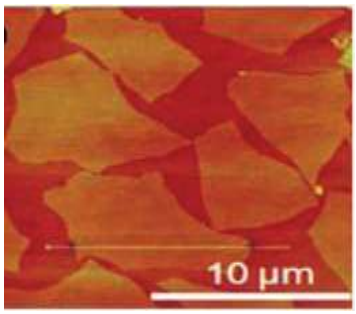

Figure 1.8 A network of graphene flakes [25].

Figure 1.9a compares ITO and fluorine tin oxide (FTO), both widely used in electronics, with a graphene flakes film of 10 nm thickness [28]. Although the conductivity of graphene sheets can be in an acceptable range, the transparency of graphene is significantly lower than that of the current commercial materials. It has been shown in Figure 1.9b that the transparency of graphene films depends on the thickness of the graphene layer. As typical for transparent electrodes of any material, thinner graphene film results in higher transparency but higher sheet resistance [29].

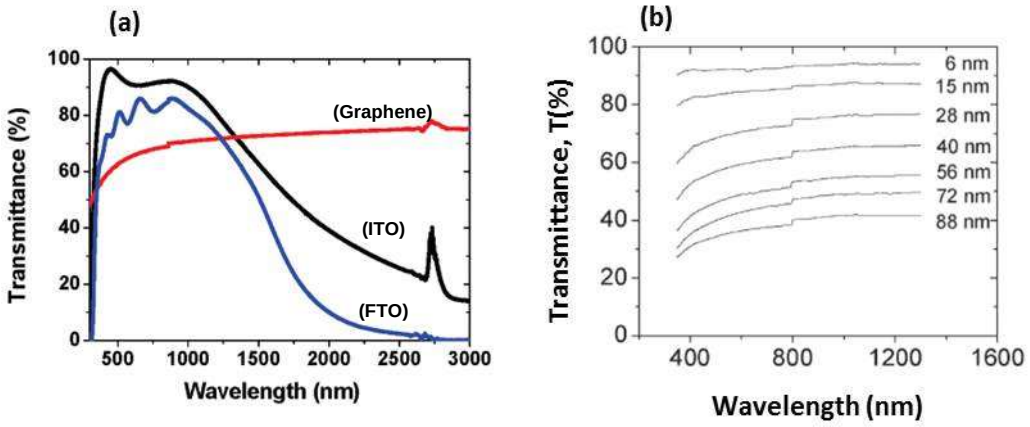

Figure 1.9 (a) Transmittance of a ca. 10 nm thick graphene flakes film (red), in comparison with that of ITO (black) and FTO (blue) [27]. (b) Transmittance spectra for thin as-produced graphitic films of various thicknesses [29].

Extensive improvements have been made in fabrication processes for graphene films and in integrating them into electronic devices. Although researchers have introduced new methods of fabricating a single sheet of graphene, such as the high temperature CVD method, the cost of this

method is relatively high [29] and the sheet resistances in these single sheets are still not low enough to be useful in most applications.

1.4. Conductive polymers

Transparent conductive polymers appeared in the mid 20th century and attracted researchers' attention because of their interesting properties like high flexibility, low cost and light weight. Several companies have been trying to use them in various devices such as touch panels and organic electronics [30]. The combination of Poly (3, 4-ethylenedioxythiophene) and poly (styrene sulfonate), known as PEDOT:PSS, is one of the most common materials on the market being used in organic electronics.

One of the major problems of conducting polymers is their instability in air due to absorption of oxygen and moisture. For example, PEDOT:PSS degrades in air in a short time. To solve this problem, extensive research is being done to synthesize more stable conducting polymers. Recently, Fujitsu company has used a type of polythiophene, which is more stable in air, for their organic touch panels [30]. In addition to stability, another major problem is that the conductivity of transparent conductive polymers is low and can therefore not replace ITO in many applications. One possibility is to combine conducting polymers with other materials such as graphene and nanostructured metals to enhance the conductivity [31,32].

1.5. Metal nanostructured electrodes

Because of the low conductivity of CNT films, graphene, and transparent conducting polymers, metal nanostructures are an appealing alternative. Metals have the highest conductivity of all types of materials. However, because of the very low transparency of metals to visible light, fabrication of transparent metallic electrodes was not easy until recent decades. Since the emergence of nanotechnology and nanostructured materials, fabricating transparent electrodes

using metallic structures has become easier. Metal nano-grids, thin metal films (of less than 10 nm thickness) and random meshes of metal nanowires are three common structures used to make transparent electrodes [9].

1.5.1. Metal thin films and grids

Thin metal films with thicknesses on the order of a few nanometers are fairly transparent to visible light, but they still have lower transparency than other materials for the same sheet resistance. Figure 1.10 illustrates the sheet resistances and transparencies of Cr and Ni thin films of various thicknesses [33]. In addition to the low transparency and conductivity values, metallic thin film deposition happens at ultrahigh vacuum by DC sputtering, which has a high manufacturing cost [9].

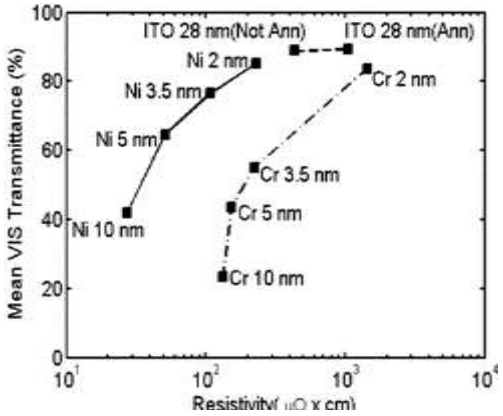

Figure 1.10 Average optical transmittance vs. electrical resistivity for Cr and Ni films compared to unannealed and annealed ITO films [33].

Metal nano-grids are patterned by complex fabrication processes such as electron beam lithography. Figure 1.11 shows an example of a nano-grid structure. These structures can provide sheet resistances of 6.5 Ω/□ with 95% transparency, values that are competing with the performance of ITO [34]. However, high surface roughness, and the intricacy and cost of fabrication are the major drawbacks of using metal nano-grid structures.

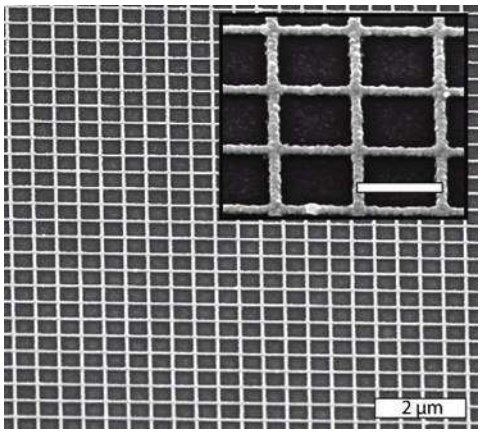

Figure 1.11 Scanning electron microscopy (SEM) image of a silver grid transparent electrode, patterned by beam lithography [34].

1.5.2. Metal nanowire electrodes

Metal nanowires are considered to be a 1D nanostructure; they have the shape of a wire, where the diameter is typically less than 100 nm, and their length is 1 µm or more. Metal nanowires such as copper or silver can be synthesized in solution, and then deposited on transparent substrates such as glass or plastic to create a random conductive mesh. These films are similar to CNT films, except in this case all wires are metallic. The mesh transparency can reach 90% for a sheet resistance below 10Ω/□, which makes the transparency and conductivity similar to that of ITO and thus suitable for transparent electrode applications [35]. Figure 1.12 show a random network of transparent electrode based on silver nanowires with various densities of nanowires. Sheet resistance and transparency of the films can be controlled by varying the density of the deposited solution to get specific properties [35]. As is the case for most transparent electrodes, there is a trade-off between transparency and conductivity: denser films of nanowires are more conductive but less transparent.

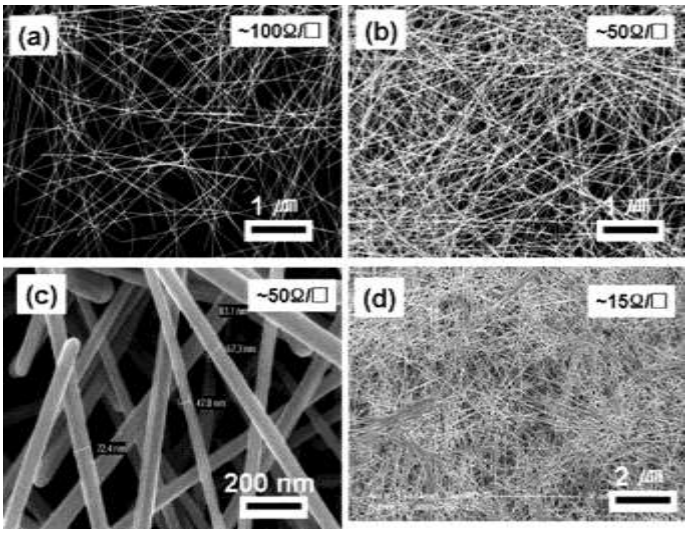

Figure 1.12 SEM images of Ag NW films with different densities. The different densities of Ag NW films lead to different sheet resistances: (a) 100, (b), (c) 50, and (d) 15 Ω /□. The diameters of the Ag NWs are in the range of 40-100 nm [35].

Simple and cheap fabrication, high transparency, and low sheet resistance are advantages of metal nanowire structures. And although silver is an expensive element, so little of it is used in a nanowire film that material costs are lower than ITO. Moreover, the nanowire electrodes are mechanically flexible. They are also much more transparent in the infrared (IR) range than ITO which makes them more suitable for multi-junction solar cells and other applications where transparency in the IR is required. A solution of silver nanowires can be deposited in atmosphere using simple and inexpensive deposition methods like spin coating [36], spray coating [37], and Meyer rod coating [35]. Silver is one of the most promising nanowire electrode materials since silver has the highest conductivity amongst metals. Moreover, silver nanowire films can be fabricated either at room temperature [38], or at low annealing temperatures [35], which make them compatible with plastic substrates in producing flexible electrodes.

Figure 1.13 compares silver nanowire electrodes with other alternatives. So far, silver nanowire electrodes show superior performance compared to graphene and CNTs.

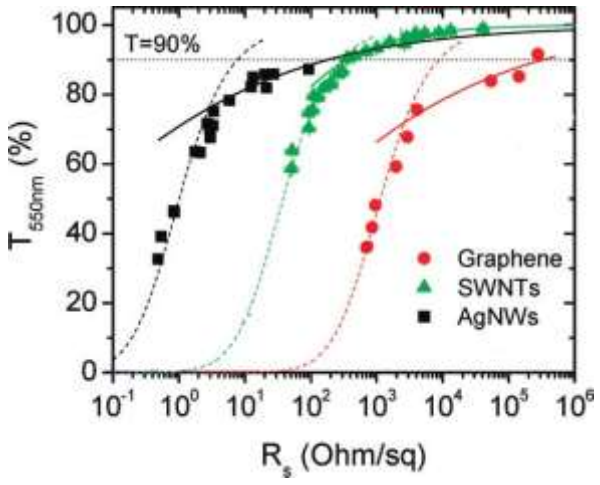

Figure 1.13 Transmittance as a function sheet resistance for three alternatives [39].

Copper nanowires are also being used for transparent conductors since copper is cheaper than silver and has high conductivity. Reported copper transparent electrodes show superior performance than CNTs but not as good as silver nanowires and ITO [40]. The main concern of using copper nanowires

is their instability in air due to the fact that copper reacts with atmospheric oxygen and the reaction speeds up at elevated temperature. Thus, the copper nanowires have to be annealed in a neutral atmosphere like hydrogen tube furnace or vacuum furnace, which increases complexity of fabrication processes, and also likely need to be passivated to prevent oxidation during the use of the electrodes [41].

1.5.3. Synthesis of silver nanowires

Silver nanowires can be synthetized in solution with the polyol method. In this method, an ethylene glycol (EG) solution of poly (vinyl pyrrolidone) (PVP) and NaCl is heated to 170 ^{o}C and a mixture of $AgNO_3$ and EG is added gradually. Adding $AgNO_3$ into the solution lead to creation of Ag^{+}, which results in formation of nanoparticles due to homogenous nucleation [42]. The PVP has a strong interaction with {100} facets and passivates these surfaces, which slows down the addition of silver onto these surfaces. The interaction of PVP with {111} facets,

however, is weaker. Thus, {111} facets grow faster in [110] direction [42], which results in a 1D wire structure [43]. This method results in pentagonal shape silver nanowires, including a 5-fold grain structure as shown in Figure1.14. The sidewalls are {100} planes. The two ends of the nanowires are bounded by {111} facets [43].

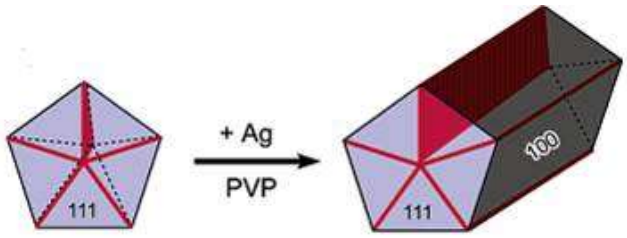

Figure 1.14 Schematic illustration of silver nanowires grown in solution by the polyol method [43].

1.5.4. Silver nanowire electrode challenges

Although films of silver nanowires are inexpensive, flexible, and have desirable transparency and conductivity values, there are some problems that need to be addressed before these electrodes can be used in commercial devices. Firstly, the surface roughness of nanowire mesh is too high to integrate it in many electronic devices. After the deposition process, some nanowires stick out of the surface and some of them lie on top of each other which increases surface roughness to a couple hundred nanometers [31]. Most applications need the surface roughness to be much less. For example, because of the low mobility of organic materials, the active layers in organic solar cells are quite thin (usually between 50 – 200 nm) and rough electrodes cause shorting [1,44]. Recently, some methods have been introduced to reduce surface roughness of the electrodes, like laminating silver nanowire films onto a soft material and making a polymer-nanowire composite [35,45]. Figure 1.15 shows surface roughness of a silver nanowire electrode before and after mechanical pressing. Although current methods have reduced the surface roughness, more improvements need to be done to decrease it further to

make those electrodes practical for organic solar cells and displays. The issue of surface roughness will be addressed in my own work in subsection 2.5.

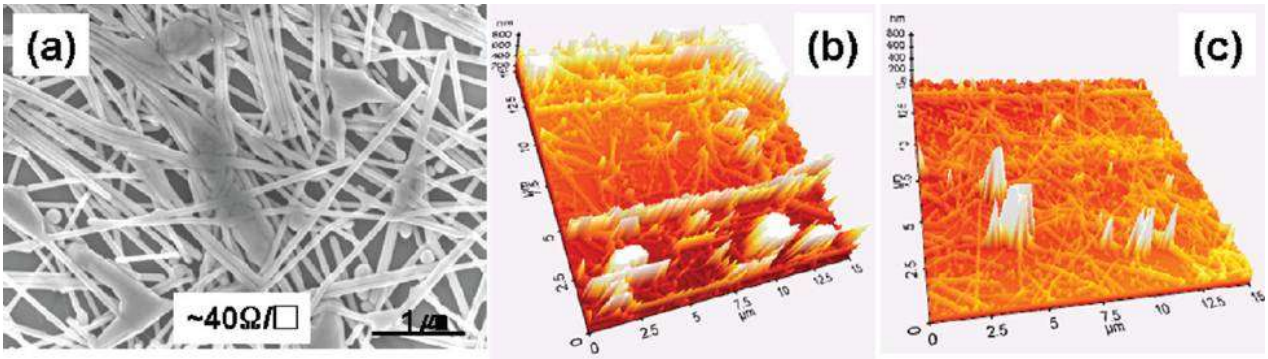

Figure 1.15 (a) SEM image of a Ag NW network after mechanical pressing; AFM images of the Ag NW network (b) before and (c) after pressing. The pressing significantly improves the smoothness. The surface roughness decreases from 110 to 47 nm after mechanical pressing [31].

A second problem, which has not received much attention up to this point, is the stability of silver nanowires over long periods of time. For example, silver is known to be susceptible to electromigration, where the flow of current causes the gradual movements of ions in a conductor. As illustrated in Figure 1.16, the flow of current through a silver nanowire can result in a void and hillock structure on two ends. This particular study was carried out on single crystalline nanowires [46], but the effects of this phenomenon have not been investigated for nanowires synthesized by the polyol process, which have grain boundaries, and not for meshes of nanowires. In addition to electromigration, it is also known that nanowires are unstable at temperatures as low as 200 °C or perhaps even less [47]. In Chapter 3, I will report on the results of experiments to access the stability of nanowire electrodes, report characterization results which help determine the cause of the instability, and provide suggestions for improving the stability of silver nanowire transparent electrodes.

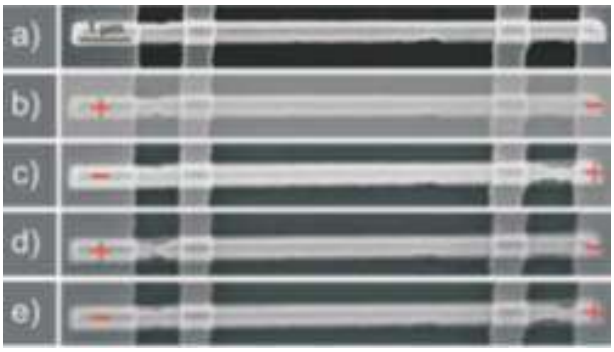

Figure 1.16 SEM image of electromigration effects due to current flow of 18-22 mA in single-crystalline silver nanowires [46].

1.6. Organization of this thesis

A method of silver nanowire transparent electrodes fabrication is reported in Chapter 2 and the electrode characteristics are discussed and compared with those of other reports. Results of a new method to reduce the surface roughness are also illustrated in Chapter 2.

This thesis also contributes to this area by investigating the instability of silver nanowire electrodes under current flow and investigates failure mechanisms (Chapter 3). Suggestions for how these electrodes can be better designed for improved longevity are given. In Chapter 4, a new application of silver nanowire, transparent heaters, is introduced. Lastly, I summarize my work in Chapter 5 and give suggestions for future work.

Chapter 2

Fabrication and characterization of silver nanowire transparent electrodes

This chapter describes a method for fabricating silver nanowire transparent electrodes and shows their optical and electrical characteristics. The performance of the fabricated electrodes is compared to that of the other reports. Silver nanowire films flexibility is also discussed and a new method of roughness reduction is introduced.

2.1 Introduction

2.1.1 Solution deposition methods

Solution synthesized silver nanowires are dispersed in an alcoholic solvent such as isopropyl alcohol (IPA), ethanol or methanol and can be deposited on various substrates using solution deposition methods. Figure 2.1 illustrates the various solution deposition methods that exist to deposit solutions into thin films or patterns. Spin coating is the most popular method for lab-scale samples due to its simplicity and reproducibility. However, for large-scale fabrication, other methods like spray coating, doctor blade coating, or wire-wound metering rod (Mayer rod) coating are more suitable and used more frequently in industry. Since transparent electrodes need to be fabricated in large-scale eventually, I chose the Mayer rod coating method, which is compatible with roll-to-roll techniques and more convenient for industry. This method is inexpensive and easy to use, just one wire-wound rod is enough for fabrication, so there is no need for any complex equipment. Moreover, using this method, the solution is distributed uniformly on the substrate

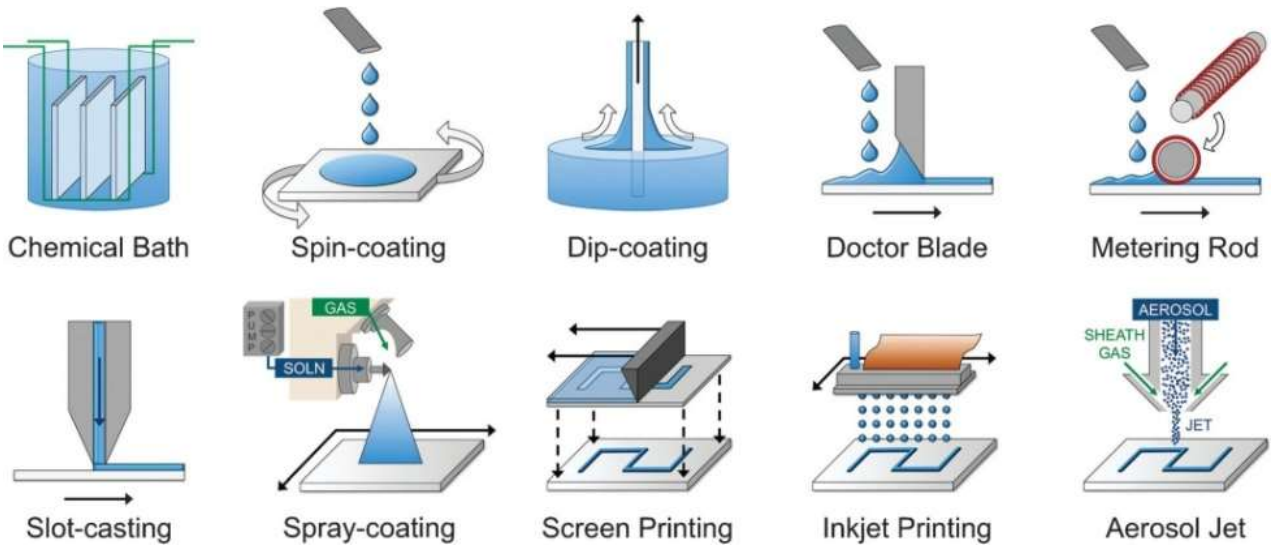

Figure 2.1 Various solution deposition methods [48]

Figure 2.2 shows the schematic of a Mayer rod. The diameter of the wound wire determines the thickness of the deposited solution.

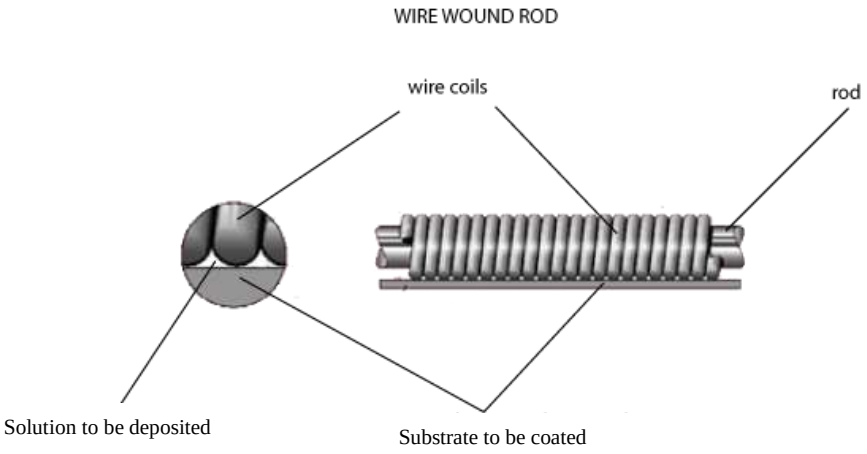

Figure 2.2 Structure of a Mayer rod [49]

2.1.2 Transparency

When light encounters an object, the incident light can be transmitted, absorbed or reflected by the object. The ratio of transmitted light to the incident light is defined as transmittance of the object, which is usually shown in percentages. Transmittance of an object can vary in response to

the wavelength of the incident light. Thus, when we report transmittance of an object the corresponding wavelength needs to be mentioned. All transmittances stated in this thesis are in reference to the substrate (i.e. do not include the transmittance of the glass or plastic) unless otherwise stated.

The total transmittance consists of two parts: specular (or direct) and diffusive. Specular transmittance represents the transmitted light travelling in the same direction as the incident light. This transmittance can be measured using the default setup of a spectrophotometer, where the detector is placed behind the object in-line with the source of the light. Figure 2.3 shows a schematic set up of a spectrophotometer for measuring specular transmittance. Diffusive transmittance represents transmitted light scattered by the object. To measure this part, an integrating sphere is needed, which collects all transmitted light including diffusive and specular. A schematic of such an integrated sphere is illustrated in Figure 2.4.

Figure 2.3 Schematic set-up of spectrophotometer for measuring specular transmittance

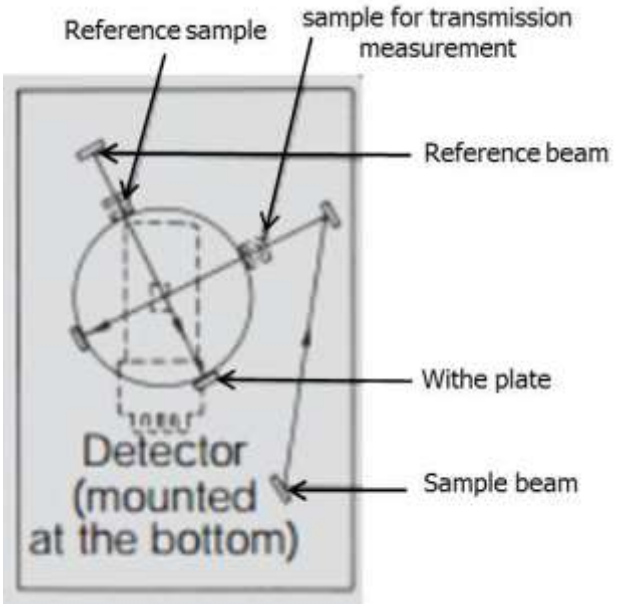

Figure 2.4 Schematic set up of using an integrated integrating sphere to measure both diffusive and specular transmittance [50]

For samples such as plain glass and ITO electrodes, diffusive transmittance is not significant since they do not scatter light. However, silver nanowire electrodes do scatter a portion of the incident light. Although scattered light results in hazy-looking electrodes, which are not good for display applications, these electrodes can benefit solar cell applications by increasing the path length of the incoming light, thereby increasing absorption and efficiency.

2.1.3 Sheet resistance

Resistivity is one of the elementary parameters of a conducting material. The symbol ρ with the unit Ω•cm represents the resistivity of a material. Resistance is related to resistivity through:

$$R = \rho \frac{L}{Wt},$$

where L is the length of the sample, and W and t are the width and thickness of the sample. Since the thicknesses of films are often difficult to measure, sheet resistance is defined to represent resistance per square area of a thin film with the unit Ω/□ (Ohms per square) and is given by

$$R_s = \frac{\rho}{t}$$

So,

$$R = R_s \frac{L}{W}$$

Thus, the total resistance of a film is proportional to the number of squares that can be drawn on the conducting surface area. Figure 2.5 shows a top view of two typical resistors with the same sheet resistance. Although their sizes are different, the numbers of drawn squares are equal. Thus, the total resistance for both resistors would be the same.

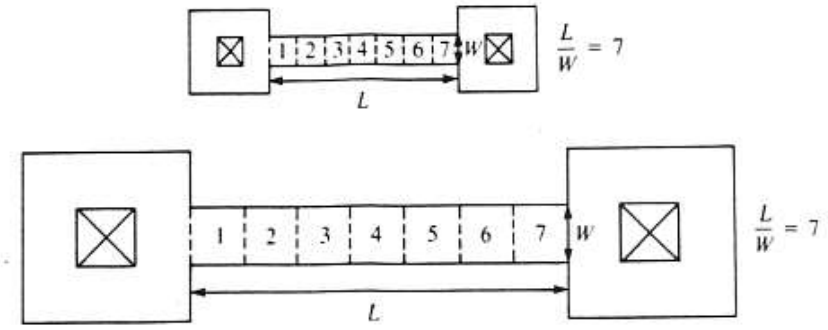

Figure 2.5 Two resistors with the same sheet resistance and total resistance [51]

2.2 Fabrication of silver nanowire transparent electrodes

Silver nanowires dispersed in ethanol were purchased from Blue Nano Inc, with an average diameter of 90nm and average length of 25 μm. The solution of nanowires needs to be deposited uniformly on a substrate. Proper concentration was found by diluting initial the as-received concentration (10 mg/ml) into various lower concentrations and depositing them on the glass substrates (Microscope cover glass purchased from Fisher Scientific, Inc). The 5 mg/ml solution

is illustrated in Figure 2.6, and of those tested it provides the best uniformity and sheet resistance on the substrates.

Figure 2.6 Silver nanowires solution with concentration of 5 mg/ml

Mayer rod size-10 and 20 were purchased from R. D. Specialities Inc. The size of the Mayer rod represents the thickness of the deposited wet film. Uniformity of the deposited layer was better for Mayer rod size 10, which made a wet layer with a thickness of 22.86 microns. Thus, 51 microliters of the solution is enough to make a layer of coating that covers the entire surface of a 50mm × 45 mm substrate. The required solution was dropped along one side of the substrate using a pipette, and then the Mayer rod was rolled from one side to the other to distribute the solution uniformly over the entire surface. Figure 2.7 illustrates the Mayer rod coating process schematically and realistically.

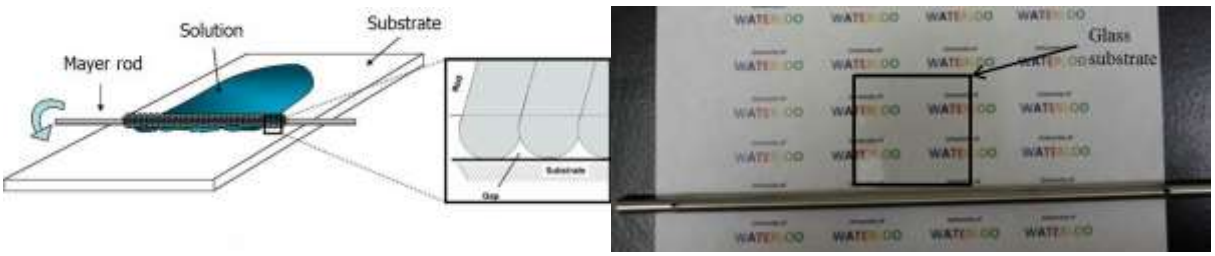

Figure 2.7 (a) Schematic illustration of the Mayer rod coating method [52], (b) Mayer rod and glass substrates for fabrication of transparent electrode

The coated layer was dried in air for 5 minutes. Additional layers can be deposited after the first layer to reduce the sheet resistance. Desired sheet resistance and optical transmittance can be achieved by controlling the number of deposited layers. After deposition, the resistance of the films was high because the overlapping nanowires were not in good contact with one another. Therefore, the films were annealed to fuse the overlapping nanowire junctions, which greatly reduced the sheet resistance. After testing several annealing temperatures and times, it was found that annealing at 200 °C for 30 minutes resulted in the lowest resistance. Higher temperatures or longer times caused the nanowires to break up and thus resulted in lower resistances. After the annealing step, two strips of copper tape were applied to the two ends of each electrode to facilitate measurement of the electrode's resistance. Figure 2.8 illustrates an electrode that has 4 deposited nanowire layers with a sheet resistance of 12 Ω/□ and 91% transmittance at 550nm.

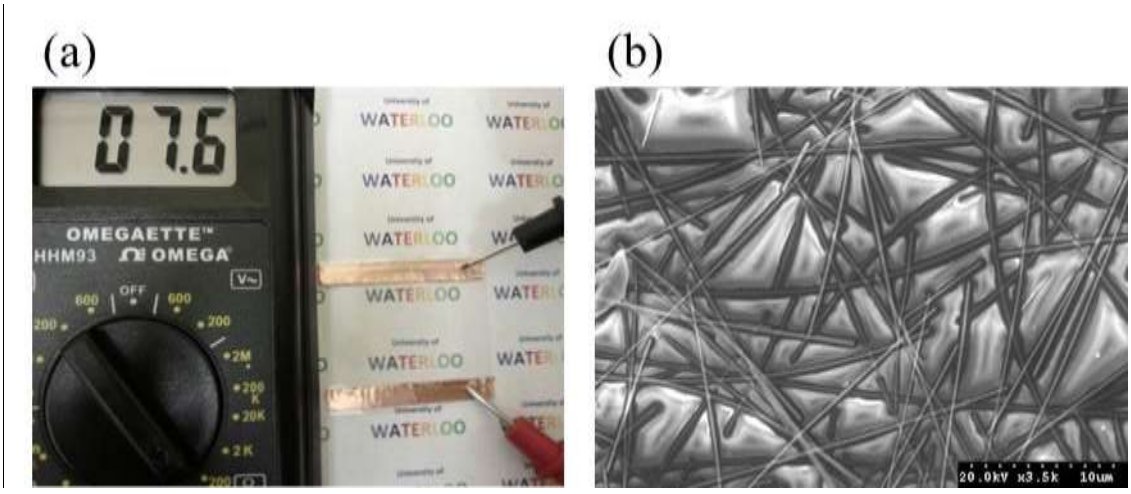

Figure 2.8 (a) Fabricated silver nanowire transparent electrode (b) SEM image of silver nanowire film on glass substrate

2.3 Characterization of silver nanowire transparent electrodes

2.3.1 Transmittance and sheet resistance

The most critical characteristics of a transparent electrode are its sheet resistance and transmittance. Sheet resistance of the electrode can be measured with either a 4-point probe machine or a multimeter. In the latter method, sheet resistance is calculated by multiplying measured resistance by the width to length ratio (W/l), according to the definition of sheet resistance. For instance, resistance of the sample in Figure 2.8a is measured as 7.6 Ω and the W/L ratio is 1.57. Thus, its sheet resistance is 12 Ω/□. Both methods were used on several samples and resulting sheet resistances were very similar.

Transmittance of the electrode was measured with a UV-2501PC Shimadzu spectrophotometer. Specular transmittance can be measured using the default spectrophotometer setup. However, an integrated sphere is needed to measure both specular and diffusive transmittances. Two samples with various sheet resistances and transmittances were prepared by controlling the number of deposited layers, and both their specular and their diffusive and specular (total) transmittances were measured for comparison. Figure 2.9 shows spectra of the samples with various sheet resistances either including (Figure 2.9a) or excluding their substrates (Figure 2.9b). A higher concentration of silver nanowires on the substrates results in lower sheet resistance and transmittance. In addition, as illustrated in Figure 2.9a, higher concentration leads to more scattering of the incident light. In this case, the sample with sheet resistance of 65 Ω/□ scatters about 6% of the incident light. However, this amount increases to more than 10% for the sample with sheet resistance of 12 Ω/□. This is because the lower resistance electrode has a higher density of nanowires, and thus scatters more.

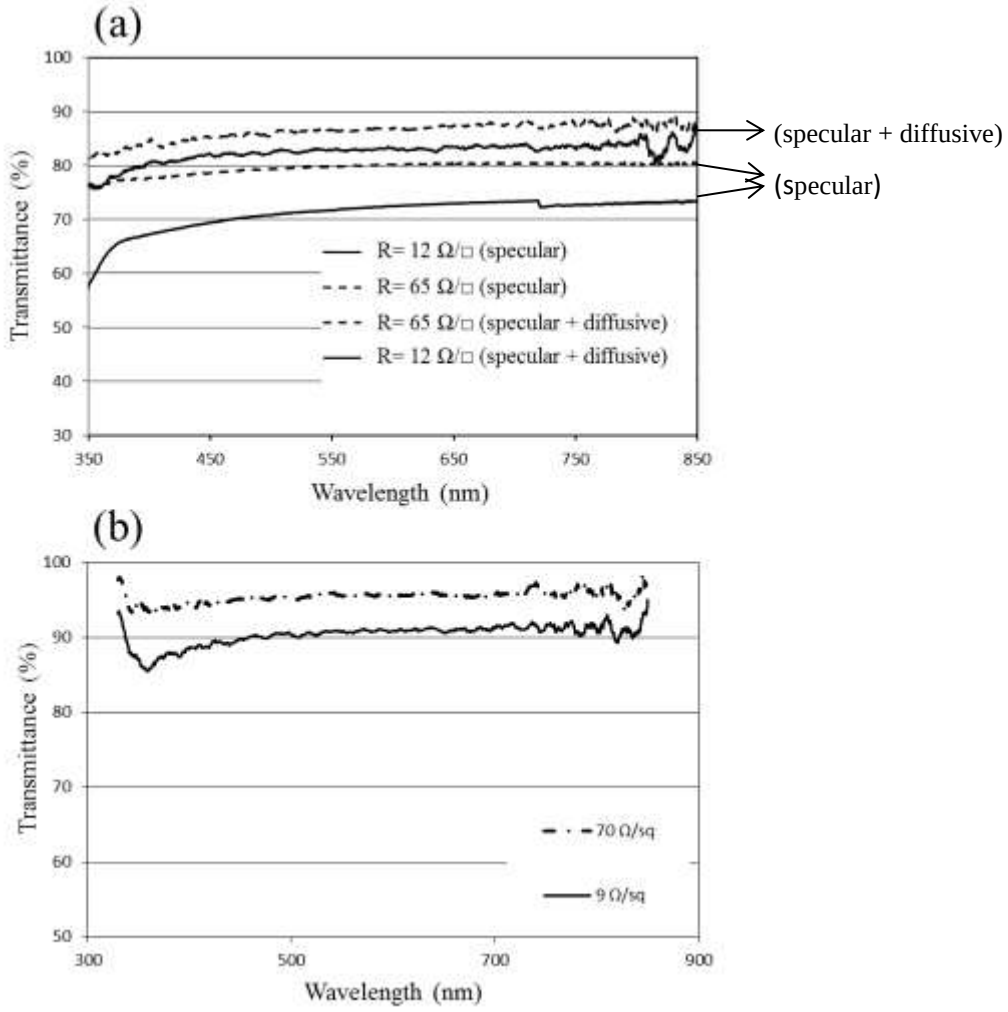

Figure 2.9 (a) Transparency vs. wavelength of two silver nanowire transparent electrodes including the glass substrates (transmittance of the plain glass is 91% at 550nm) (b) Transparency (specular + diffusive) of the electrodes excluding the glass substrate (glass is used as a reference)

2.3.2 Data comparison

As mentioned, several alternatives have been introduced for ITO replacement. Figure 2.10 compares the characteristics of my silver nanowire electrodes with that of some of the alternative materials and commercial ITO. Because high transparency and low resistance is desired, the closer the data points are to the top left corner, the better. Results indicate that the silver

nanowire transparent electrodes have better performance than the competing alternative materials and match or are very close to commercial ITO.

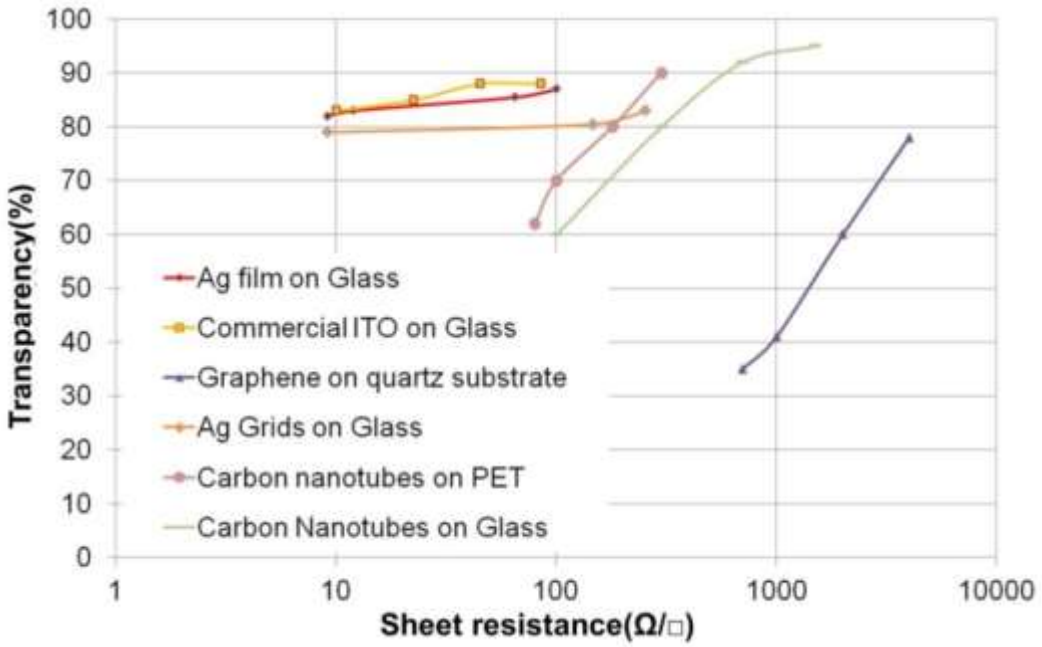

Figure 2.10 Transparency versus sheet resistance for several transparent electrode materials. The data for the silver nanowire electrodes are from my own experiments and references for the remainder of the data in the plot is from [53]–[57].

2.3.3 Cost of silver nanowire films

Silver is an expensive metal, however, the amount of the silver that is used for fabrication of a silver nanowire electrode is not significant. The price of pure silver is about $0.4 for the amount of silver used in one meter square of an electrode with a sheet resistance of 10 Ω/□ and 91% transmittance at 550 nm. Because additional reactants, like ethylene glycol, are required to synthesize silver nanowires, the cost to produce silver nanowires is more than the cost of silver alone. The material cost of silver nanowire films with the same resistance and transparency as stated above using commercial silver nanowire solutions (eg. from Blue Nano Inc.) is about $80 per meter square. However, if the nanowire solution is produced in the lab, the cost of silver

nanowire synthesis is $32.58/g and thus, the material cost of the films would be $12 per meter square for a 10 Ω/□ electrode, and less for electrodes with higher sheet resistances.

2.4 Flexibility of silver nanowire electrodes

Silver nanowires need to be deposited on a plastic substrate, such as PET or PEN, to enable flexible transparent electrodes. PET films with 700 gauge (178 μm) thickness were purchased from Dupont Teijin Films Inc. A solution of silver nanowires was deposited on the PET film as described in the fabrication section. The electrodes were annealed at 100 °C for 30 min since higher temperature can damage the PET substrate. Because this annealing temperature was lower than the ideal temperature, the nanowire junctions were not well fused and the sheet resistance of the PET electrodes was higher than that of glass after annealing. To reduce the sheet resistance, the PET electrodes were pressed in a mechanical press. Several electrodes were prepared in the same manner, and pressures of 10 MPa, 20 MPa, 30 MPa and 40 MPa were applied to the different electrodes. It was determined that 30 MPa resulted in the lowest sheet resistances. A film of silver nanowires with a sheet resistance of 9 Ω/□ and transmittance of 91% at 550 nm was fabricated with this method, which is almost the same performance as the annealed silver nanowire films on the glass substrates. To the best of our knowledge, this is the best performance of flexible silver nanowire electrodes.

Several papers have shown the flexibility of silver nanowire transparent electrodes [58–60]. The sheet resistance of spray coated and patterned silver nanowire transparent electrodes increased more than 30% under a 120° and 140° bending angle, respectively [58-59]. However, our samples show only 0-5% increase in sheet resistance under 140° bending angle and with bending radius of 10 mm as it is illustrated in Figure 2.11. Once the sample is returned to its original flat

state, the resistance returns to its original value. Moreover, the sheet resistance did not change after bending 100 times. It can be concluded that the PET silver nanowire electrodes are promising for flexible electronics.

Figure 2.11 Resistance changes of flexible silver nanowire transparent electrode under a 140° bending angle (10 mm bending radius).

2.5 Surface roughness

As discussed in the Chapter 1, high surface roughness of silver nanowire electrodes is a major problem. Atomic force microscopy (AFM) was used to measure the roughness of an as-deposited silver nanowire electrode. The RMS (Root Mean Square) surface roughness was 60nm over 10 μm × 10 μm area. Figure 2.12b shows the height of the surface along a linear scan. At some points, there are 3 nanowires on top of one another and since the nanowires have a diameter of 90 nm, the maximum peak-to-valley height was nearly 300 nm.

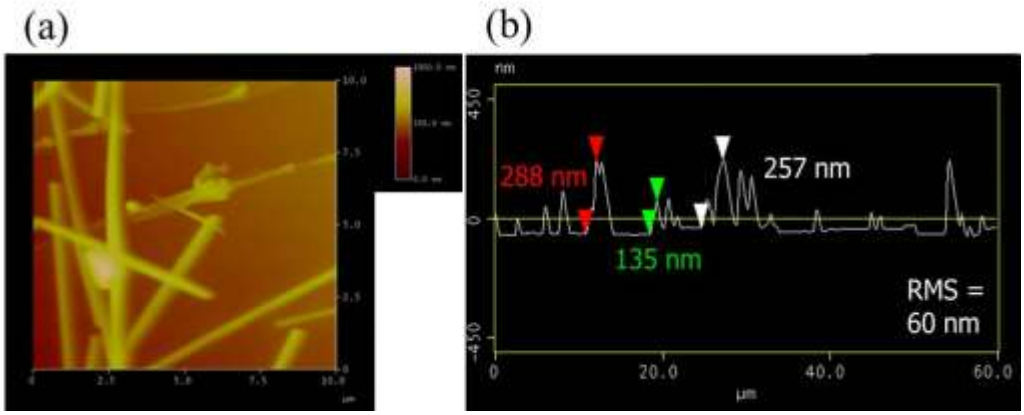

Figure 2.12 (a) AFM image of as-deposited film of silver nanowire (b) The height of the surface along a linear scan

To reduce surface roughness, I first tried to reduce surface roughness by pressing nanowires on PET in the same manner as described in the last subsection. Figure 2.13 shows the electrodes surface before and after pressing. Although surface roughness decreases more than 4 times after pressing (in Figure 2.15), it is still far from the required smoothness for most of the applications. For example, in most of the organic thin film electronics the RMS should be less than 10 nm and the pick to valley distance must be less than 20 nm (depends on the thickness of the organic layer).

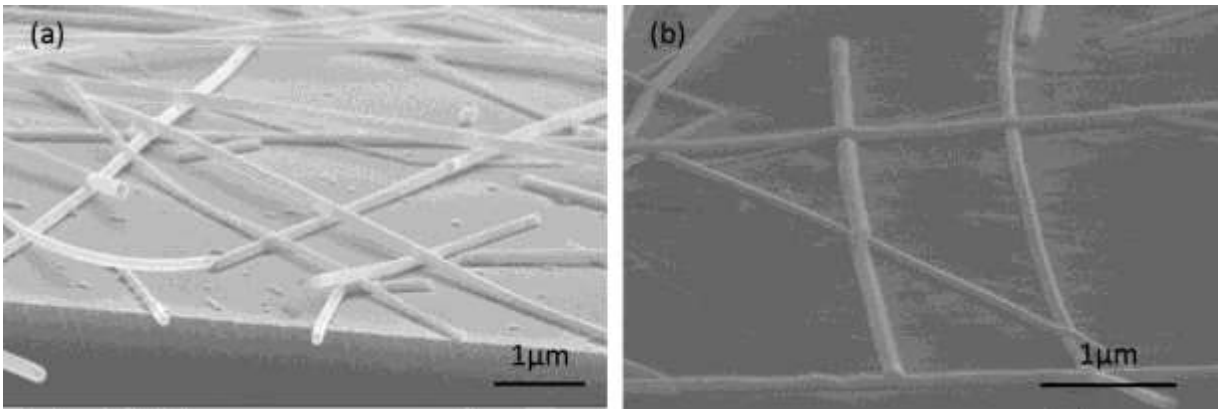

Figure 2.13 SEM image of a silver nanowire electrode (a) after deposition (b) after pressing.

This problem of nanowire electrode surface roughness has been addressed by other research groups with two different approaches. One group used PEDOT:PSS, a transparent and

conductive polymer, to fill the spaces between the nanowires [61]. Surface roughness was successfully reduced, however, because of the high roughness of the nanowire film a PEDOT:PSS thickness of more than 125 nm is required. At these thicknesses there is a significant reduction in transparency due to the limited transparency of the conductive polymer. The second approach is to deposit a non-conductive but transparent polymer on top of the nanowire electrode, and then peeling off the polymer-nanowire composite [62].The manufacturing of this method would be complex and costly, however.

I developed a new method to reduce the surface roughness of silver nanowire electrodes which do not have the drawbacks mentioned in the previous paragraph. Like the second method mentioned, I used a transparent and non-conductive soft polymer, either SU-8 or PMMA, to fill the space between the nanowires. However, instead of depositing the polymer on top of the nanowire electrode, the nanowire film was instead pressed into the soft polymer. The nanowire film was embedded into the top surface of the polymer and thus the polymer did not have to be conductive, nor did the polymer-nanowire composite have to be peeled off the substrate. Because I was not restricted to using a conductive polymer, this allowed me to select a polymer that was much more transparent than a conducting polymer such as PEDOT:PSS. A SU-8 layer with thickness of 1mm has more than 95% transmittance at 550nm [63].

In this method, a soft polymer layer was spin coated onto a substrate, and then the coated film was placed on a hot plate slightly below the baking temperature of the polymer. Thus, the coated polymer was neither soft nor completely hard. In this condition, silver nanowires were deposited on the substrate and then pressed in a mechanical press with a pressure of 30 MPa. Figure 2.14 shows the schematic of this process. This process results in embedding silver nanowires into the polymer and reducing surface roughness dramatically

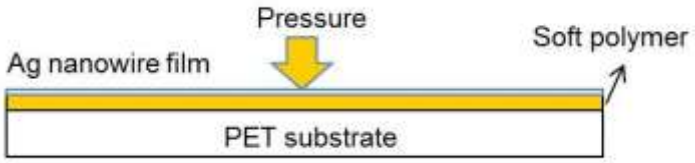

Figure 2.14 Schematic of the embedding process of silver nanowires into a soft polymer film

Figure 2.15 shows AFM results for the pressed sample versus embedded nanowires. This surface is smooth enough for many applications even though further optimization is needed to decrease the roughness further to reach to the required roughness for thinner devices.

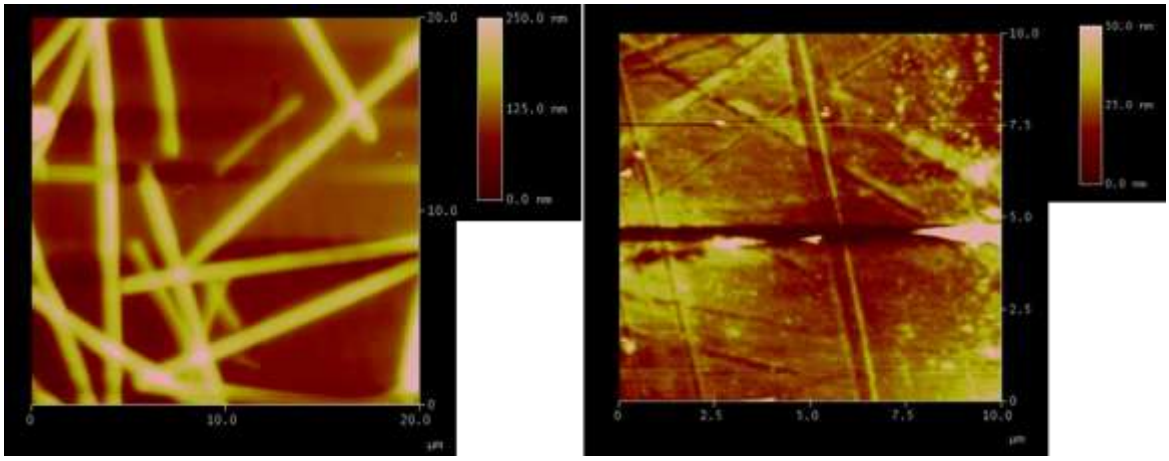

Figure 2.15 AFM image of pressed film of silver nanowire (left), and embedded silver nanowires on a soft polymer (right)

2.6 Device integration

I used the fabricated silver nanowire electrodes in different devices and applications. In Chapter 4, silver nanowire electrodes are used as transparent heaters, which is a new application of these electrodes. Moreover, the electrodes were used in organic solar cells as the anode layer at the top of an inverted device as illustrated in figure 2.16. Leanne Murphy, a Master's student from Chemical Engineering department of the University of Waterloo helped me to make the device and collected the required data. In this structure, light can be shone through both sides, which

can enhance the efficiency of the solar cells and open the possibility for partially transparent solar cells which could be used on windows for example.

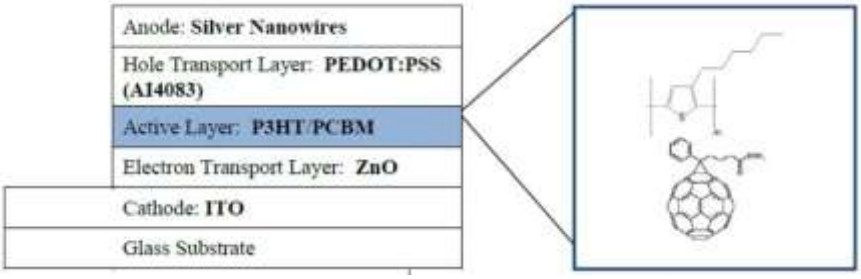

Figure 2.16 Photovoltaic device structure used for the fabrication of inverted devices.

Figure 2.17 shows the I-V curve of the solar cell for both sides. A fill factor (FF) of 25% and power conversion efficiency (PCE) of 0.2% were obtained from the silver side of the device. Although the initial results were not satisfactory and far from the ideal range, the fabrication process was not optimized and was done only as a proof-of-concept. It shows that the silver nanowire electrodes can be used in organic solar cells.

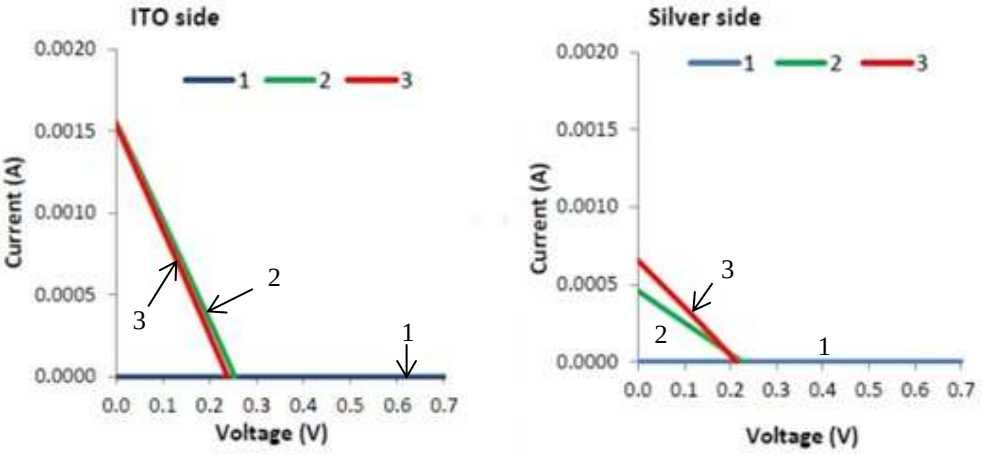

Figure 2.17 I-V curves through the ITO side and the silver nanowire side of the top illuminated solar cells prepared using silver nanowires and P3HT/PCBM

The silver nanowire electrodes were also used in switchable privacy glass by a group of nanotechnology undergraduate students of University of Waterloo. In this device, a liquid crystal

solution was injected between two pieces of glass coated with silver nanowire electrodes. The transparency of the liquid crystal solution was altered by applying a voltage across the two electrodes.

Chapter 3

Instability of silver nanowire transparent electrodes under current flow

In this chapter, we show that when silver nanowire electrodes conduct the current at levels encountered in organic solar cells, the electrodes can fail in as little as two days. Electrode failure is caused by Joule heating which causes the nanowires to breakup and thus create an electrical discontinuity in the nanowire film. More heat is created, and thus failure occurs sooner in more resistive electrodes and at higher current densities. Suggestions to improve the stability of silver nanowire electrodes are given. These results were summarized in a paper submitted in March 2013 [98].

3.1. Introduction

There are numerous reports about the promising device characteristics of organic solar cells using silver nanowire electrodes [64,65]. Silver nanowires are known to oxidize and corrode over a period of months in air [66], however, there are no studies on the stability of the nanowire electrodes during use (i.e. when they are conducting current). In contrast to ITO where current conducts throughout the entire area of the film, in nanowire electrodes electronic transport occurs only through the metal wire pathways, and these nanowire pathways have diameters less than 100 nm. Because of this, although the current densities generated in organic solar cells are relatively low (on the order of 10 mA/cm^2, with the best performing devices generating about 17 mA/cm^2 [67]), the resulting current densities in the nanowires are very high. For example, if we assume half the nanowires in 12 Ω/□ silver nanowire electrodes participate in current conduction, a solar cell current density of 17 mA/cm^2 would result in an approximate current

density in the nanowires of 4×10^4 A/cm^2 [68]. For comparison, this same current flowing through a 250 nm thick ITO film results in a current density of 10^3 A/cm^2, more than an order of magnitude less.

In this chapter, it is shown that at current density levels incurred in organic solar cells, silver nanowire electrodes fail in a matter of days. We report how parameters such as sheet resistance and current density affect the time to failure, as well as characterize the electrodes to investigate the failure mechanism.

3.2. Experiment

Silver nanowires electrodes were fabricated and characterized as described in chapter 2. To investigate the effects of current flow through the electrodes, a DC power supply was used to pass a constant current across the electrodes. Current was conducted until the electrodes failed, which we define as the point when the DC power supply reached its maximum of 30 V and thus could no longer maintain the constant current. The voltage across the electrodes and the surface temperature were monitored continuously throughout the experiment using computer data collection. For the temperature measurement, a flat leaf-style thermocouple was used. The electrodes were soon afterwards imaged with SEM, for which a thin coating of gold on the sample was required to prevent electron charging. Transmission electron microscopy (TEM) samples were prepared by mechanically rubbing the electrodes onto copper grids overlayed with ultra-thin amorphous carbon. Both bright-field images and energy dispersive spectroscopy (EDS) spectra were obtained in the TEM.

For comparison purposes, additional nanowire electrodes were prepared but no current was passed across them. Rather, one electrode was left in air and its sheet resistance was monitored

over the period of one year. Other electrodes were annealed in an atmospheric furnace each at various temperatures and times. These electrodes were imaged in the SEM at various stages to see how the electrode morphology evolved throughout the annealing process.

3.3. Results and discussion

3.3.1 Electrode failure measurements

An SEM image of a prepared nanowire electrode is shown in Figure 3.1a. The transparency of all electrodes was nearly constant across all visible wavelengths (Figure 2.9), as similarly found by other groups [69,70,71]. The electrodes prepared for the stability experiments had sheet resistances ranging from 12 Ω/□ (with a corresponding transparency of 91% at a wavelength of 550 nm) to 37 Ω/□ (with a transparency of 94% at 550 nm). Figure 3.1b shows the evolution of the voltage and surface temperature of a 12 Ω/□ nanowire electrode as 17 mA/cm^2 of current was passed across it. As was typical with all samples measured, the voltage (and therefore resistance) gradually increased with time, and then suddenly jumped to 30 V once the electrode failed. The power dissipated in the electrode is P = IV, so with a constant current and a gradually increasing voltage, the surface temperature gradually increased over time as well until electrode failure.

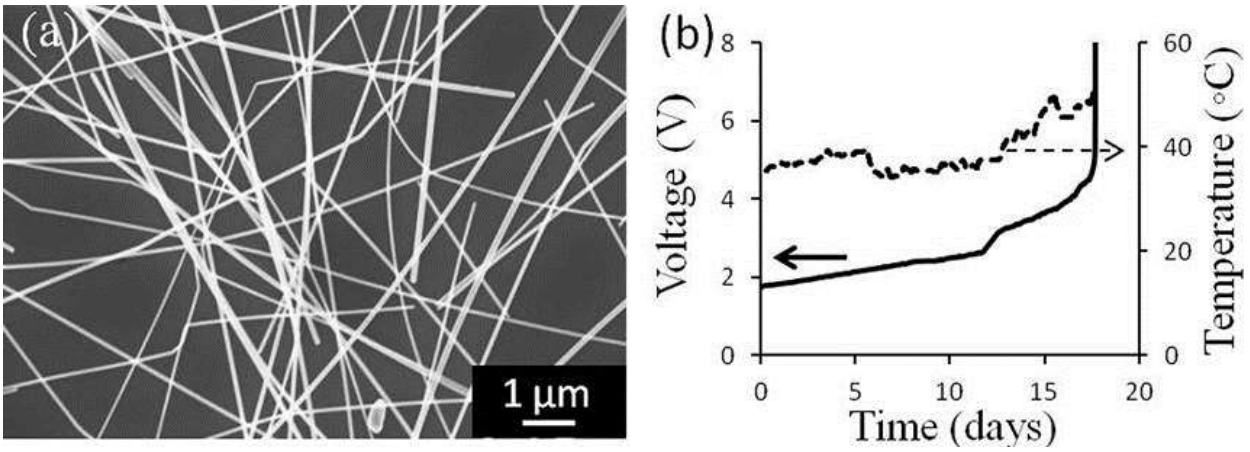

Figure 3.1 (a) SEM image of an as-prepared electrode. (b) Voltage and surface temperature of a 12 Ω/□ sample when a constant current density of 17 mA/cm^2 was applied across the electrode

Figure 3.2a shows that under a constant current density, electrodes with a higher sheet resistance fail more quickly. Higher sheet resistance electrodes have sparser nanowire networks, and thus the current density in the individual nanowires is higher than in lower resistance electrodes. Joule heating is also higher in more resistive films, since $P = IV = I^2R$. The surface temperatures immediately preceding electrode failure of the four samples measured for Figure 3.2a, from the lowest to highest sheet resistance, was: 55 °C, 70 °C, 100 °C, and 102 °C.

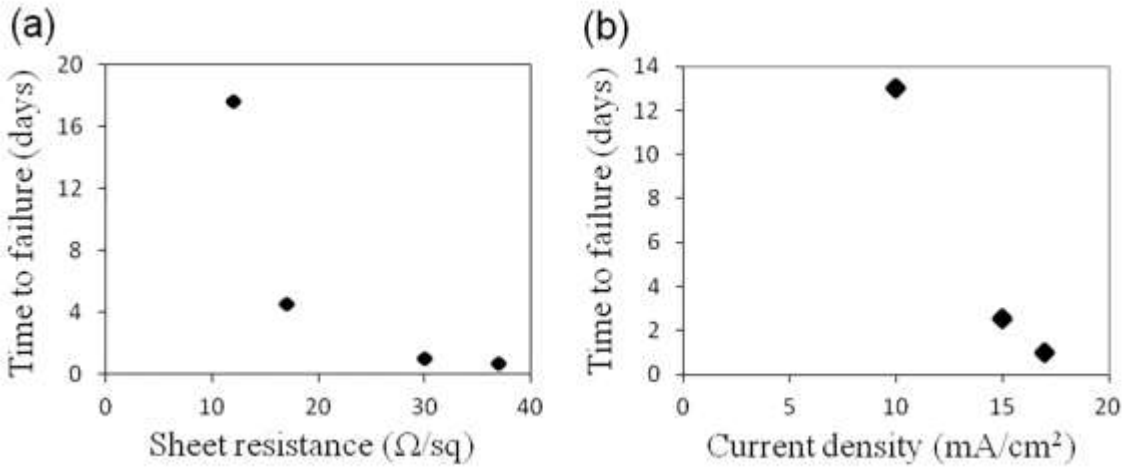

Figure 3.2 (a) The number of days to failure versus sheet resistance, when conducting 17 mA/cm2 across samples with different resistances. (b) The relationship between the number of days to failure and current density, as measured with three different 30 Ω/□ electrode

Figure 3.2b illustrates that for nanowire electrodes with the same sheet resistance, a higher current density results in a shorter lifetime. Similar to above, a higher current density results in higher currents through the individual nanowires and more Joule heating. The temperature of the electrode preceding failure for the three current densities applied in Figure 3.2b, from lowest to highest current density, was: 50 °C, 74 °C, and 100°C.

In the comparison sample, where a nanowire electrode was left in air without current flow, the sheet resistance only increased by 10% after three months. After one year, however, the resistance was 6 orders of magnitude higher than its original value.

3.3.2 Failure mechanism characterization

Typical SEM images of the electrodes after failure are shown in Figure 3.3. In contrast to the smooth nanowire sidewalls observed in the as-prepared films, nanoparticles were now present on the nanowire surfaces for the sample with a sheet resistance of 12 Ω/□. The size of the created nanoparticle are measured between 30-60nm from the SEM images. However, since the samples are coated with a 20 nm thick gold layer, the actual size of the nanoparticle are smaller than they appear. In some locations on the sample, as in Figure 3.3b, nanowires were broken up into discontinuous segments. Enough nanowires in the electrode were broken up such that there was no longer a continuous electrical pathway across the film.

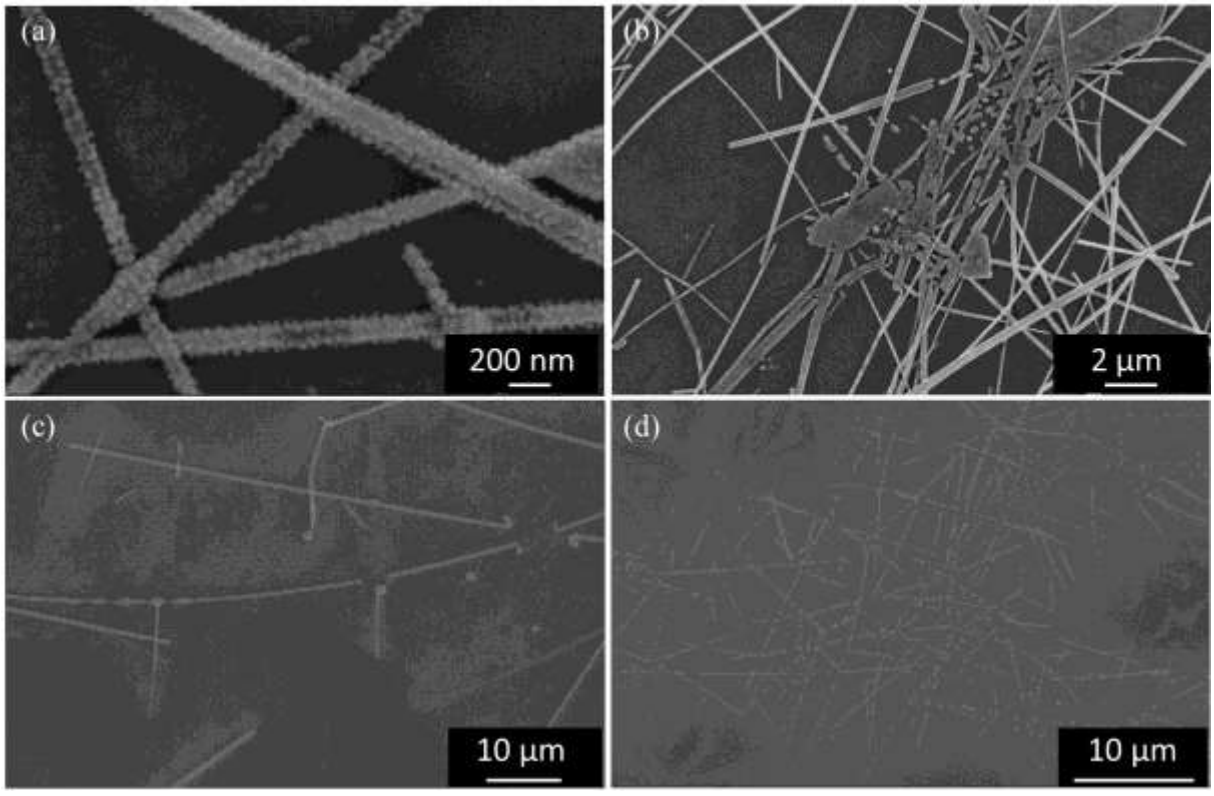

Figure 3.3 SEM images of a silver nanowire electrode after a constant current density of 17 mA/cm^2 was passed across it (a,b) for 17 days with a sheet resistance of 12 Ω/□, and (b,c) for 17 hour with a sheet resistance of 36 Ω/□

.

Figure 3.3 c and d shows SEM images of the electrode after failure with higher sheet resistance under the same current density as the sample in Figure 3.3 a and b. In this case the shapes of the nanowires are completely changed into spherical forms in some locations, which may be due to the higher temperature resulting from the higher current density passing through individual nanowires.

Although silver is susceptible to electromigration at the current densities and temperatures encountered in these electrodes [72], the SEM images are not indicative of the voids and hillocks that are characteristic of electromigration [11–14]. Rather, our study suggests that it is the instability of nanowires at elevated temperatures which is the reason for the electrode failure. As mentioned in the experimental section, nanowire electrodes were annealed at various temperatures without current flow. Figure 3.4 shows SEM images of nanowire during annealing for 17 days at 100 °C and 150 °C. Even at a temperature as low as 100 °C, nanoparticles formed on the surfaces of the nanowires The samples annealed at 100 °C were removed from the furnace every few days to take images throughout the annealing process. The resulting images show that the size and density of nanoparticles increased with increasing annealing time. At 150 °C, nanoparticles also formed and the nanowires eventually broke up into discontinuous segments (Figure 3.4d).

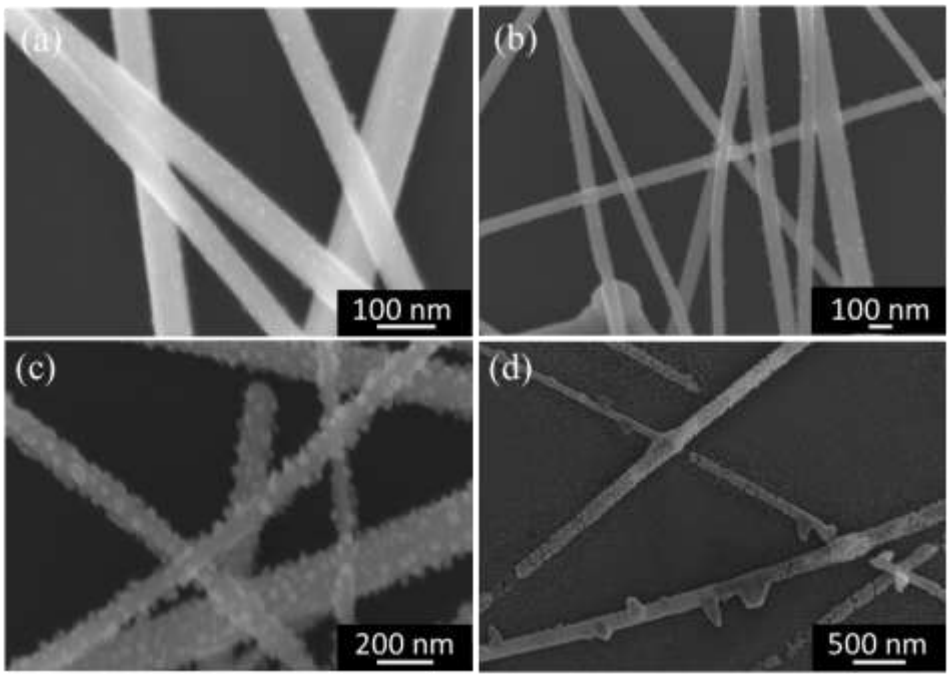

Figure 3.4 SEM images of silver nanowire electrodes annealed on a glass substrate for (a) 7 days, (b) 14 days, and (c) 17 days at 100 °C, and for (d) 17 days at 150 °C.

In addition, silver nanowires were annealed at higher temperature for a short time to investigate the effect of higher temperature on silver nanowire structures. Figure 3.5 shows optical microscope images of the silver nanowires after annealing at 300 °C for one and half hours. The nanowire were melted or turned into spherical shapes after a short time.

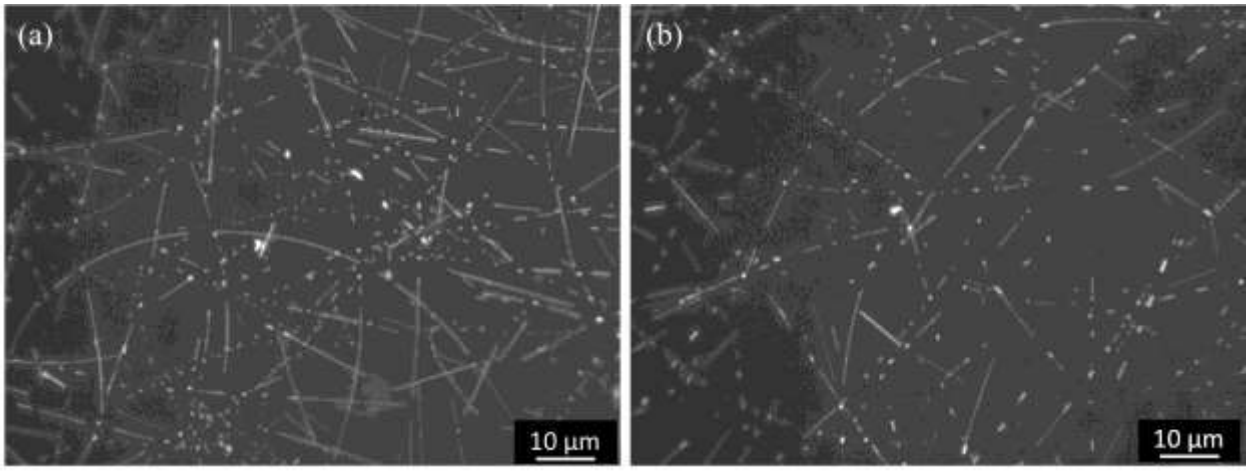

Figure 3.5 silver nanowires annealed at 300 °C (a) for half an hour (b) for one and half hour.

As noted in the section above, when current is passed through a nanowire electrode the temperature is elevated due to Joule heating. Although the surface temperature of the electrodes was around or below 100 °C while conducting current, the temperature of the nanowires themselves are intuitively higher than the average surface temperature, particularly at the resistive junctions where two nanowires overlap. The annealing experiments showed that nanowire networks in air at modest temperatures are unstable; nanoparticles first form and then the nanowires eventually break up and become electrically discontinuous. Thus, in the case of current conduction, the temperature of the nanowires rise due to Joule heating and the instability of the nanowires at these temperatures causes the electrodes to fail. Comparing the time to failure of the 12 Ω/□ electrode under 17 mA/cm^2 of current flow to the time for the nanowires in the annealed samples to breakup, we estimate the temperature of the nanowires themselves in this particular case was between 100 and 150 °C. In addition, the resulting structures of the silver nanowire, annealed at 300 °C, are similar to the 36 Ω/□ silver nanowire electrodes under 17 mA/cm^2 of current flow, which failed after 17 hours (Figure 3.3d).

Elechiguerra et al. found that silver nanowires synthesized by the polyol method corrode in the atmosphere [77]. Rather than corroding by reacting with oxygen, silver corrodes due to reduced-sulfur gases present in the air. They observed that after three weeks, silver sulfide (Ag_2S) nanoparticles started to form on the surface of the nanowires and after six months, some of the nanowires became discontinuous. In our experiments, nanoparticles and breakage occur much faster. Corrosion is greatly enhanced at elevated temperatures [16]. EDS spectra were taken from the nanoparticles decorating the surface of the nanowires after electrode failure (Figure 3.6). Other than the carbon and copper signals originating from the TEM grid, only silver and sulphur were detected. The ratio of silver to sulphur content was 9:1. The presence of sulphur

indicates that the electrodes may have failed due to the corrosion of the nanowires in the atmosphere at the elevated temperatures caused by Joule heating.

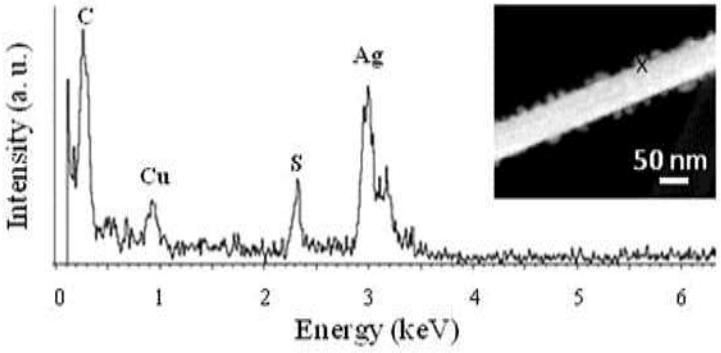

Figure 3.6 Energy dispersive spectrum of a nanoparticle formed on a silver nanowire after electrode failure. The x indicates the location where the measurement was taken. Sulfur was detected in the nanoparticles indicating corrosion of the silver.

Alternatively, or addition to corrosion, another reason for the breakup of the silver nanowires at increased temperatures could be attributed to the high surface energy of the nanowires. Nanowires have a large surface-area-to-volume ratio, and the sidewalls of the nanowires used in the electrodes are all {110} planes [79], which are not the lowest energy planes in an FCC material. At elevated temperatures, atomic diffusion is increased and kinetic limitations to reconstruction can be overcome. Silver nanobelts and nanowires of other metals have been shown to fragment at temperatures far below their bulk melting temperatures due to Rayleigh instability [80], [81] and a similar phenomenon may be occurring here.

3.3.3 Relevance to nanowire electrode design

The experimental results indicate that steps must be taken to improve the longevity of nanowire electrodes under current flow before they are suitable for use in organic solar cells. In a flexible organic solar cell, the substrate underneath the transparent electrode is typically a plastic such as polyethylene terephthalate (PET) or polyethylene naphthalate (PEN), and organic materials are

deposited on top of the electrode. PET and PEN are permeable to gas [82], as are many of the common small molecules or polymeric materials in organic solar cells [83], and so these materials will likely not prevent corrosion. Researchers are developing organic solar cell materials with low permeability to gas [84,85]. Alternatively, encapsulation of the organic solar cell [86,87] may prevent the corrosion of the silver nanowire electrode. Another option is to passivate the silver nanowires with a conductive coating. Ahn et al. showed that a graphene oxide coating, which is impermeable to gas molecules, reduced, but did not completely prevent, the increase of sheet resistance of silver nanowire electrodes when annealed at 70 °C in high humidity over one week [88]. A better passivation will likely be required.

Larger diameter nanowires would take longer to corrode, and also have smaller surface-area-to-volume ratios and would thus be more stable at elevated temperatures. Another potentially helpful strategy would be to synthesize and deposit films of silver nanowires which have low energy {111} facets. Also, alternative metallic nanowires that are less susceptible to corrosion could be considered, such as cupronickel nanowires [89]. Our results also indicate the importance of keeping current densities low and using low resistance nanowire electrodes, which are unfortunately less transparent.

3.4. Conclusions

The data in this chapter shows that at current levels generated in organic solar cells, silver nanowire electrodes fail in an unacceptably short time. Electrodes with higher sheet resistances, and electrodes subject to higher current densities, fail more quickly. The reason for electrode failure is attributed to elevated temperatures caused by Joule heating. Design factors such as passivation, electrode sheet resistance, and nanowire diameter need to be considered before silver nanowire electrodes will be useful as an ITO replacement in organic solar cells.

Chapter 4

Silver nanowire transparent heaters

In this chapter, silver nanowire transparent heaters are introduced as a new application of silver nanowire electrodes. The performance and characterization of the transparent heaters are illustrated and compared with conventional transparent heaters and other new alternatives. We show that the heating performance of silver nanowire heaters is better than those of ITO and CNT heaters, lower power is required to reach to the same surface temperature. Moreover, a voltage as low as 6 V heats the surface up to 100 ^{o}C.

4.1 Introduction

Transparent heater films have applications in many areas such as window defrosters, maintaining the required temperature for liquid crystal display operation, goggle defrosters, and various military and medical applications. ITO thin film heaters are commercially available on the market. However, as mentioned in previous chapters, because of the disadvantages of ITO like high cost and brittleness, researchers are trying to introduce new transparent heaters based on other materials such as graphene and carbon nanotubes [90–93].

In addition to their cost, flexibility, and ease of fabrication, the thermal conductivity and power consumption of the heaters are also critical characteristics that need to be considered. ITO has low thermal conductivity in the order of 8-12 W/m•K [94]. In comparison, silver has a thermal conductivity of 400-440 W/m•K which is 50 times higher than that of ITO [95]. The thermal conductivity of CNT and graphene are about one order of magnitude higher than that of silver, and this high conductivity results in fast heating and cooling [95]. However, if a higher surface temperature is required, the higher sheet resistance of graphene and CNT films necessitates that a

higher voltage be applied or that a film with a low transmittance (and therefore lower resistance) be used. Such is not the case with silver nanowire electrodes. A heater's performance is determined by calculating its power consumption for generating a particular surface temperature. A high performance heater needs less power to reach the required surface temperature.

Silver nanowire transparent electrodes not only have relatively high thermal conductivity but also have low sheet resistance and high transmittance. Thus, transparent heaters based on silver nanowires can perform with very low voltages and provide high transmittance. Recently, fabrication of silver nanowire transparent heaters has been reported elsewhere [96], which preempted our efforts to publish the first report on this application but confirmed our results.

4.2 Experiment setup

Transparent electrodes with various sheet resistances were fabricated either on PET or glass substrates with the size of 40 mm × 50 mm, as described in Chapter 2. For the PET samples, a pressure of 30 MPa was applied to enhance the sheet resistance of the films, as mentioned in Chapter 2. Figure 4.1 shows the schematic of experimental setup. A flat leaf-style thermocouple was attached to the backside of the substrate (opposite side from the nanowire film) and the temperature data was collected using a digital thermometer connected to a computer. The surface temperature was recorded every second during the experiment. A constant voltage was applied for 600 seconds across the copper strips using a DC power supply, creating a flowing current which was also recorded. Then the power supply was disconnected from the electrode and surface temperatures were still monitored to plot the cooling trend.

The total transmittance (specular and diffusive) of the films were measured using an integrating sphere and a spectrophotometer, and the sheet resistances were measured using either a multi-meter or 4-point probe system, as described in Chapter2.

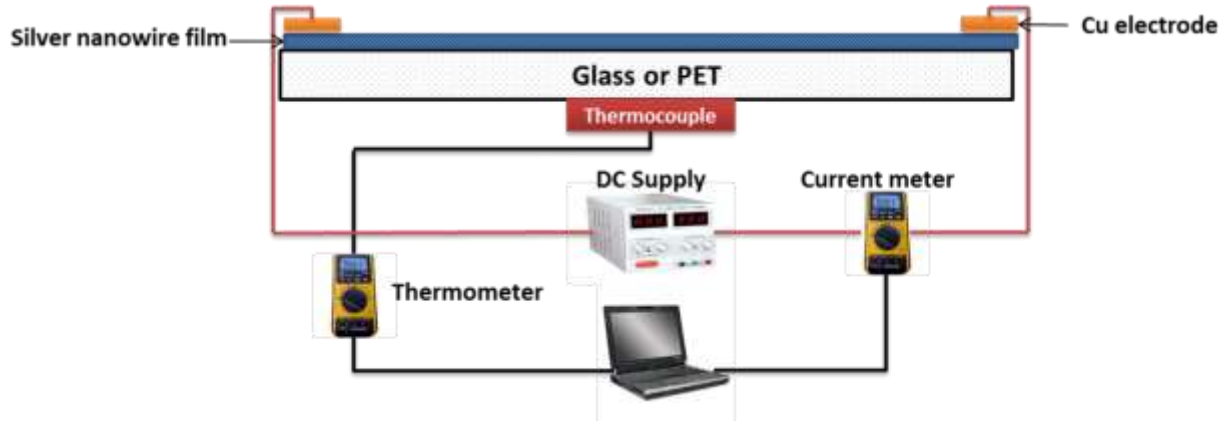

Figure 4.1 Schematic setup of experiment for measuring the transparent heater performance

The power consumption was calculated using the following equation:

$$P = \frac{V^2}{R}$$

where P is the power consumption in Watts, V is the applied voltage, and R is the film's resistance, which can be calculated by dividing the voltage by the recorded current. The equation indicates that for the same power consumption, a lower sheet resistance results in lower required voltage. Power densities were calculated for each sample by dividing the calculated power by the surface area of the heater.

4.3 Results and discussion

Heating and cooling trends of the silver nanowire transparent heaters under various applied voltages, on PET and glass substrates, are shown in Figure 4.2. This figure shows that almost all of the heaters reach their steady state temperature after 200 seconds. In addition, Figure 4.2a shows that the surface temperature of the heater on a PET or a glass substrate reached about 80 ^{o}C with a low voltage of 6 V. For comparison, the surface temperature of ITO and CNT film

heaters with sheet resistance of 392 Ω/sq and 356 Ω/sq reached 31 °C and 85 °C under 12 V, respectively [91,92]. A graphene film heater with a sheet resistance of 43 Ω/sq reached close to 100 °C at 12 V [92], which thus has better performance than that of ITO and CNT. However, here we found that silver nanowire heaters' surface temperature, with the same aspect ratio as reported heaters, exceeds 120 °C at 12 V. Usually the required heat in most transparent heater applications is below 100 °C, so for silver nanowire electrodes with an aspect ratio of 1.25 a voltage of 6 V would be high enough.

According the reported results for ITO, a power of 0.03 W/cm^2 can heat the ITO film only to 31 °C [92]. For CNT heaters, a power of 0.65 W/cm^2 heated the film up to 55 °C [91]. Graphene heaters perform better: for a HNO_3-doped graphene heater, 0.08 W/cm^2 provides a surface temperature of about 60 °C [92]. However, fabrication process of graphene electrodes is expensive and complicated. Figure 2.2a illustrates that a power of 0.03 W/cm^2, 0.07 W/cm^2 and 0.12 W/cm^2 in the silver nanowire films can respectively generate heat up to 43 °C, 60 °C and 87 °C, which are almost similar to the results achieved by graphene heaters and superior than ITO and CNT heaters.

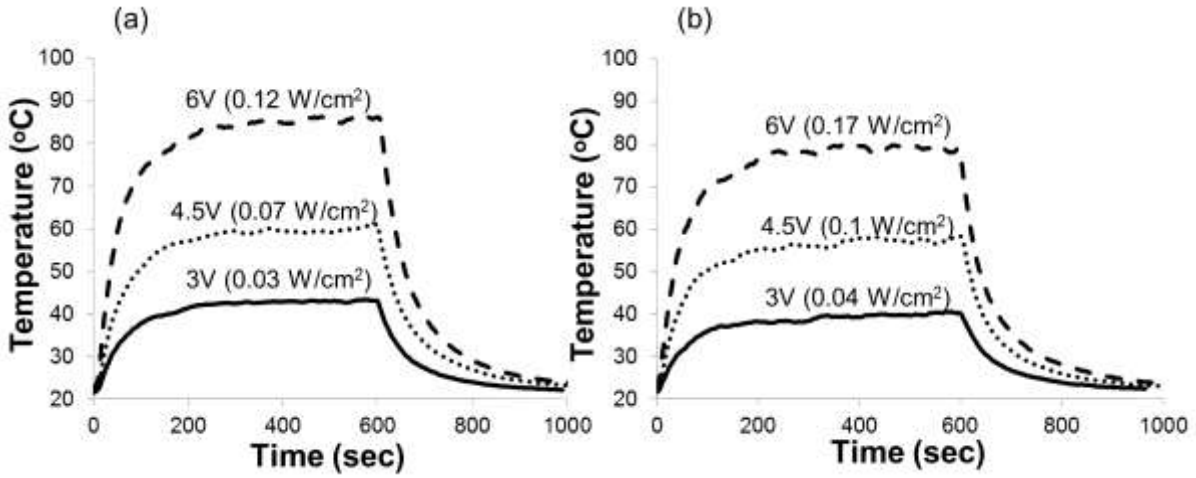

Figure 4.2 Heating profile of the transparent heaters with 92% transmittance at 550 nm (a) on PET with sheet resistance of 22 Ω/sq (b) on glass with sheet resistance of 15 Ω/sq. The labelled voltages are the voltage applied across the films and the power density is stated in brackets.

As illustrated in Figure 4.2, the PET substrate heater reaches higher temperature with lower power consumption than glass substrates with the same thickness, meaning that PET substrate heaters perform better. The power densities vs. maximum surface temperature were plotted for the PET and the glass substrates for different sheet resistances, as shown in Figure 4.3. This figure confirms that for the same power density, PET heaters reach higher surface temperature. This behavior might be due to the difference in thermal conductivity of the substrates; glass thermal conductivity is about five times greater than that of PET [96,97]. Thus, heat is transferred slower in PET, resulting in higher surface temperature.

Figure 3 also shows that for the same input power, the maximum temperature at a given power density is higher for heaters with higher sheet resistance. We know that higher sheet resistance is a consequence of a lower concentration of silver nanowires. Therefore, for a given input power, each nanowire dissipates more power. According to the following thermodynamic equation, higher power consumption results in a bigger temperature change

$$Q = mc\Delta T$$

where Q is the consumed energy in Joules, and m and c are the mass of the nanowire and specific heat capacity of silver, respectively. For the same power input to a sample with low sheet resistance (due to a higher concentration of nanowires), the change in temperature of each individual nanowire would be smaller.

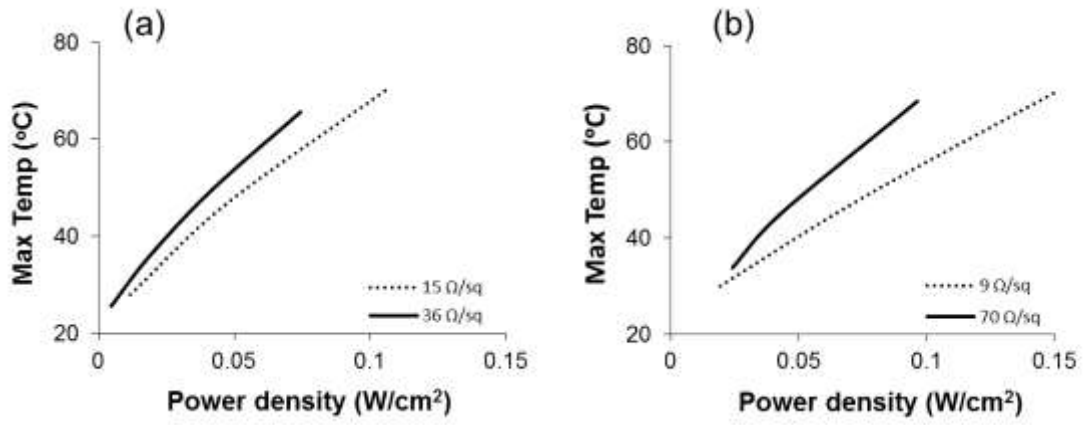

Figure 4.3 Maxiumum surface temperature vs. power density for nanowire heaters with various sheet resistances on (a) PET and (b) glass.

Figure 4.4 shows the heating and cooling trend of silver nanowire transparent heaters with various transmittances under a voltage of 6 V. As discussed in the previous paragraph, at a given power density more resistive films (and thus more transparent films) reach higher temperature. However, when the voltage is constant, as in this case, more current flows through the less resistive films (lower transparency films) which draws more power and thus generates a higher temperature. The sample with 90 % transmittance at 550 nm provides heat up to 100 $^{\circ}$C, which is promising for transparent heaters.

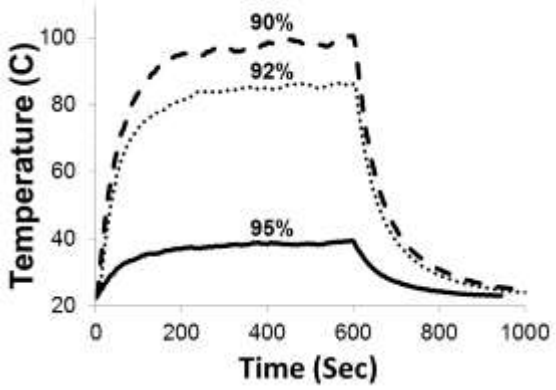

Figure 4.4 Heating profiles of the transparent heaters on the glass substrates with various transmittances under applied voltage of 6 V

To investigate the long-term performance of the silver nanowire transparent heaters, a constant voltage of 4.5 V was applied to a sample for four days and the surface temperature and resistance of the film were monitored continuously. As illustrated in Figure 4.5 the surface temperature was stable during the four days of the experiment. However, the instability of silver nanowires over longer times needs to be considered for this application as discussed in the previous chapter.

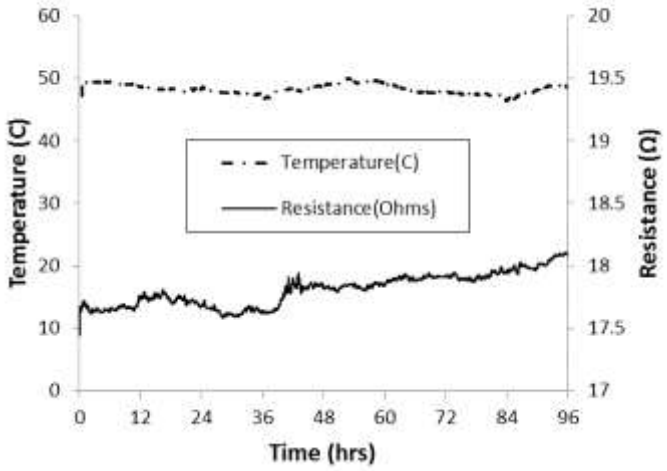

Figure 4.5 Temperature and resistance changes of a silver nanowire heater with a sheet resistance of 24 Ω/sq during 4 days of applying 4.5 V across its terminals

4.4 Conclusions

This chapter has introduced transparent heaters as a new application for silver nanowire transparent electrodes. Fabricated heaters resulted in better performance than ITO and CNT heaters due to its lower power consumption and required voltage. Moreover, the heaters with transmittances higher than 90% at 550 nm can generate temperatures of nearly 100 °C with a voltage of only 6 V with power consumption of 0.12 W/cm^2. Thus, these heaters only need a low voltage source (smaller batteries). In addition, when deposited on PET substrates, the transparent heaters are flexible which opens up new application areas compared to traditional ITO heaters.

Chapter 5
Conclusions and future work

5.1 Summary and conclusions

In this thesis, silver nanowire electrodes, which were fabricated by the Mayer rod coating method, have been shown as a promising option for ITO film replacement. The characteristics and performance of the electrodes have been illustrated and compared with alternative materials. Silver nanowire electrodes show higher conductivity and transparency than other alternative materials and exhibit performance similar to ITO films. Moreover, silver nanowire electrodes with PET substrates have the same performance as the electrodes with glass substrates and show high flexibility, less than 5% change in sheet resistance, under a 140° mechanical bending angle and after several cycles of bending.

Concerns regarding the roughness and instability of silver nanowire electrodes were addressed. Chapter 2 introduced a new method to reduce the roughness of PET silver nanowire electrodes by embedding the nanowires into a soft polymer, a process that decreased the surface roughness by more than one order of magnitude. In Chapter 3, the instability of the silver nanowires was investigated under DC current flow. We have demonstrated that the silver nanowire electrodes fail under the current flow after a short period of time. These results indicate that the failure of the electrodes is due to the instability of the silver nanowires at elevated temperatures, which is caused by Joule heating.

The electrodes have also been integrated in different electronic devices, including transparent heaters, organic solar cells, and switchable privacy glass. In Chapter 4, silver nanowire transparent heaters are introduced as a new application of the silver nanowire electrodes. The fabricated heaters perform better than the ITO and CNT heaters, consume less power to reach the same surface temperature and need low applied voltage. The effect of sheet resistance on the performance of these heaters is also discussed in this chapter. The surface temperature of a silver nanowire heater with 90% transmittance at 550 nm wavelength, reached to 100° C under an applied voltage of 6V

5.2 Future work

The study of silver nanowires and fabricated transparent electrodes can proceed in several directions. I suggest a few important directions here. Firstly, further investigation should be done on the instability of the solution-synthesized silver nanowires and possible ways to make them more stable. We need methods of passivating the surfaces of silver nanowires with conductive films so that the electrodes can operate over long lifetimes. Secondly, the silver nanowire electrodes can be integrated in and optimized for various electronic devices. For example, it is likely that the performance of organic solar cells using nanowire electrodes can be improved by optimizing the fabrication process. Thirdly, although I presented a method to reduce the surface roughness of the electrodes, for some applications the roughness needs to be reduced further so an optimization of my process or a different process should be investigated.

References

[1] F. Yakuphanoglu and R. S. Anand, “Charge transport properties of an organic solar cell,” Syn. Met, vol. 160, no. 21, pp. 2250–2254, 2010.

[2] http://www.dmccoltd.com/english/tecnical/logs/images/tec20041126_a_1.gif.

[3] http://news.thomasnet.com/fullstory/Transparent-Heater-utilizes-ITO-technology-27584.

[4] D. S. Ginley, Handbook of Transparent Conductors. Springer, 2010.

[5] B. Zhang, X. Dong, X. Xu, X. Wang, and J. Wu, “Electrical and optical properties of ITO and ITO: Zr transparent conducting films,” Mat. Sci. Semicon. Proc. , vol. 10, no. 6, pp. 264–269, 2007.

[6] S. H. Mohamed, F. M. El-Hossary, G. A. Gamal, and M. M. Kahlid, “Properties of Indium Tin Oxide thin films deposited on polymer substrates,” Acta Phys. Polonica A, vol. 115, no. 3, pp. 704–708, 2009.

[7] Fenn J, “If not ITO, then what?” presented at Soc. Vac. Coat., 2010.

[8] D. R. Cairns, D. K. Sparacin, D. C. Paine, and G. P. Crawford, “19.3: Electrical Studies of Mechanically Deformed Indium Tin Oxide Coated Polymer Substrates,” in SID Symposium Digest of Technical Papers, 2012, vol. 31, pp. 274–277.

[9] D. S. Hecht, L. Hu, and G. Irvin, “Emerging Transparent Electrodes Based on Thin Films of Carbon Nanotubes, Graphene, and Metallic Nanostructures,” Adv. Mat., vol. 23, no. 13, pp. 1482–1513, Apr. 2011.

[10] S. Iijima and T. Ichihashi, “Single-shell carbon nanotubes of 1-nm diameter,” Nature, vol. 363, no. 6430, pp. 603–605, Jun. 1993.

[11] M. S. Fuhrer, J. Nygård, L. Shih, M. Forero, Y. G. Yoon, M. S. C. Mazzoni, H. J. Choi, J. Ihm, S. G. Louie, A. Zettl, and P. L. McEuen, "Crossed Nanotube Junctions," Science, vol. 288, no. 5465, pp. 494–497, Apr. 2000.

[12] S. Xie, W. Li, Z. Pan, B. Chang, and L. Sun, "Mechanical and physical properties on carbon nanotube," Phy. Chem. Sol, vol. 61, no. 7, pp. 1153–1158, Jul. 2000.

[13] X. Wan, J. Dong, and D. Y. Xing, "Optical properties of carbon nanotubes," Phys. Rev. B, vol. 58, no. 11, pp. 6756–6759, Sep. 1998.

[14] "http://www.ppr3.go.th/carbon-nanotubes-images&page=3."

[15] B. Dan, G. C. Irvin, and M. Pasquali, "Continuous and scalable fabrication of transparent conducting carbon nanotube films," ACS Nano, vol. 3, no. 4, pp. 835–843, 2009.

[16] D. S. Hecht, A. M. Heintz, R. Lee, L. Hu, B. Moore, C. Cucksey, and S. Risser, "High conductivity transparent carbon nanotube films deposited from superacid," Nanotechnology, vol. 22, no. 7, p. 075201, 2011.

[17] Z. Wu, "Transparent, Conductive Carbon Nanotube Films," Science, vol. 305, no. 5688, pp. 1273–1276, Aug. 2004.

[18] P. N. Nirmalraj, P. E. Lyons, S. De, J. N. Coleman, and J. J. Boland, "Electrical Connectivity in Single-Walled Carbon Nanotube Networks," Nano Lett, vol. 9, no. 11, pp. 3890–3895, 2009.

[19] Z. Li, H. R. Kandel, E. Dervishi, V. Saini, A. S. Biris, A. R. Biris, and D. Lupu, "Does the wall number of carbon nanotubes matter as conductive transparent material?," App. Phy. Lett, vol. 91, no. 5, p. 053115, 2007.

[20] D.-W. Shin, J. H. Lee, Y.-H. Kim, S. M. Yu, S.-Y. Park, and J.-B. Yoo, "A role of HNO_3 on transparent conducting film with single-walled carbon nanotubes," Nanotechnology, vol. 20, no. 47, p. 475703, 2009.

[21] H. Z. Geng, K. K. Kim, K. P. So, Y. S. Lee, Y. Chang, and Y. H. Lee, "Effect of acid treatment on carbon nanotube-based flexible transparent conducting films," J. Am. Chem. Soc, vol. 129, no. 25, pp. 7758–7759, 2007.

[22] N. Saran, K. Parikh, D. S. Suh, E. Munoz, H. Kolla, and S. K. Manohar, "Fabrication and characterization of thin films of single-walled carbon nanotube bundles on flexible plastic substrates," J. Am. Chem. Soc, vol. 126, no. 14, pp. 4462–4463, 2004.

[23] B. B. Parekh, G. Fanchini, G. Eda, and M. Chhowalla, "Improved conductivity of transparent single-wall carbon nanotube thin films via stable postdeposition functionalization," Appl. Phys. Lett, vol. 90, no. 12, p. 121913, 2007.

[24] C. M. Trottier, P. Glatkowski, P. Wallis, and J. Luo, "Properties and characterization of carbon-nanotube-based transparent conductive coating," J. Soc. Info. Displ, vol. 13, no. 9, pp. 759–763, 2005.

[25] A. A. Green and M. C. Hersam, "Solution Phase Production of Graphene with Controlled Thickness via Density Differentiation," Nano Lett, vol. 9, no. 12, pp. 4031–4036, Dec. 2009.

[26] K. S. Novoselov, A. K. Geim, S. V. Morozov, D. Jiang, Y. Zhang, S. V. Dubonos, I. V. Grigorieva, and A. A. Firsov, "Electric Field Effect in Atomically Thin Carbon Films," Science, vol. 306, no. 5696, pp. 666–669, 2004.

[27] H. C. Schniepp, K. N. Kudin, J.-L. Li, R. K. Prud'homme, R. Car, D. A. Saville, and I. A. Aksay, "Bending Properties of Single Functionalized Graphene Sheets Probed by Atomic Force Microscopy," ACS Nano, vol. 2, no. 12, pp. 2577–2584, 2008.

[28] X. Wang, L. Zhi, and K. Müllen, "Transparent, Conductive Graphene Electrodes for Dye-Sensitized Solar Cells," Nano Lett, vol. 8, no. 1, pp. 323–327, 2008.

[29] A. N. Obraztsov, "Chemical vapour deposition: Making graphene on a large scale," Nat. Nano, vol. 4, no. 4, pp. 212–213, 2009.

[30] "http://www.fujitsu.com/downloads/EDG/binary/pdf/find/26-1e/11.pdf," organic conducting polymers.

[31] W. Hong, Y. Xu, G. Lu, C. Li, and G. Shi, "Transparent graphene/PEDOT–PSS composite films as counter electrodes of dye-sensitized solar cells," Electrochem. Commun, vol. 10, no. 10, pp. 1555–1558, 2008.

[32] J. Zou, H.-L. Yip, S. K. Hau, and A. K.-Y. Jen, "Metal grid/conducting polymer hybrid transparent electrode for inverted polymer solar cells," Appl. Phys. Lett, vol. 96, no. 20, p. 203301, 2010.

[33] D. S. Ghosh, L. Martinez, S. Giurgola, P. Vergani, and V. Pruneri, "Widely transparent electrodes based on ultrathin metals," Opt. Lett, vol. 34, no. 3, pp. 325–327, 2009.

[34] J. van de Groep, P. Spinelli, and A. Polman, "Transparent conducting silver nanowire networks," Nano Lett, vol. 12, no. 6, pp. 3138–3144, 2012.

[35] L. Hu, H. S. Kim, J. Y. Lee, P. Peumans, and Y. Cui, "Scalable coating and properties of transparent, flexible, silver nanowire electrodes," ACS nano, vol. 4, no. 5, pp. 2955–2963, 2010.

[36] B. Krajnik, D. Piatkowski, M. Olejnik, N. Czechowski, E. Hofmann, W. Heiss, and S. Mackowski, "Fluorescence Mapping of PCP Light-Harvesting Complexes Coupled to Silver Nanowires." , Acta Physica. Polonica, Vol. 122, Issue 2, p. 259, 2012.

[37] V. Scardaci, R. Coull, P. E. Lyons, D. Rickard, and J. N. Coleman, "Spray Deposition of Highly Transparent, Low-Resistance Networks of Silver Nanowires over Large Areas," Small, vol. 7, no. 18, pp. 2621–2628, 2011.

[38] T. Tokuno, M. Nogi, M. Karakawa, J. Jiu, T. T. Nge, Y. Aso, and K. Suganuma, "Fabrication of silver nanowire transparent electrodes at room temperature," Nano Res, pp. 1–8, 2011.

[39] S. De, P. J. King, P. E. Lyons, U. Khan, and J. N. Coleman, "Size Effects and the Problem with Percolation in Nanostructured Transparent Conductors," ACS Nano, vol. 4, no. 12, pp. 7064–7072, 2010.

[40] A. R. Rathmell and B. J. Wiley, "The Synthesis and Coating of Long, Thin Copper Nanowires to Make Flexible, Transparent Conducting Films on Plastic Substrates," Adv. Mat, vol. 23, no. 41, pp. 4798–4803, Nov. 2011.

[41] A. R. Rathmell, S. M. Bergin, Y.-L. Hua, Z.-Y. Li, and B. J. Wiley, "The Growth Mechanism of Copper Nanowires and Their Properties in Flexible, Transparent Conducting Films," Adv. Mat, vol. 22, no. 32, pp. 3558–3563, 2010.

[42] S. Coskun, B. Aksoy, and H. E. Unalan, "Polyol Synthesis of Silver Nanowires: An Extensive Parametric Study," Crys. Growth Des, vol. 11, no. 11, pp. 4963–4969, Nov. 2011.

[43] Y. Sun, B. Mayers, T. Herricks, and Y. Xia, “Polyol synthesis of uniform silver nanowires: a plausible growth mechanism and the supporting evidence,” Nano Lett, vol. 3, no. 7, pp. 955–960, 2003.

[44] Z. Yu, L. Li, Q. Zhang, W. Hu, and Q. Pei, “Silver Nanowire-Polymer Composite Electrodes for Efficient Polymer Solar Cells,” Adv. Mat, vol. 23, no. 38, pp. 4453–4457, 2011.

[45] B. E. Hardin, W. Gaynor, I. Ding, S. B. Rim, P. Peumans, and M. D. McGehee, “Laminating solution-processed silver nanowire mesh electrodes onto solid-state dye-sensitized solar cells,” Org. Elec, vol. 12, no. 6, pp. 875–879, 2011.

[46] B. Stahlmecke, F. J. Meyer zu Heringdorf, L. I. Chelaru, M. Horn-von Hoegen, G. Dumpich, and K. R. Roos, “Electromigration in self-organized single-crystalline silver nanowires,” Appl. phys. Lett, vol. 88, no. 5, pp. 053122, 2006.

[47] J. Y. Lee, S. T. Connor, Y. Cui, and P. Peumans, “Solution-processed metal nanowire mesh transparent electrodes,” Nano Lett, vol. 8, no. 2, pp. 689–692, 2008.

[48] R. M. Pasquarelli, D. S. Ginley, and R. O’Hayre, “Solution processing of transparent conductors: from flask to film,” Chem. Soc. Rev, vol. 40, no. 11, p. 5406, 2011.

[49] “http://www.holoeast.com/machines/coating/WIRE-WOUND-ROD.png.”

[50] “http://www.ssi.shimadzu.com/products/literature/Spectroscopy/UV-Vis_Accessories.pdf.”

[51] “http://www.ece.gatech.edu/research/labs/vc/theory/sheetRes.html.”

[52] B. Dan, G. C. Irvin, and M. Pasquali, “Continuous and scalable fabrication of transparent conducting carbon nanotube films,” ACS Nano, vol. 3, no. 4, pp. 835–843, 2009.

[53] J. Zou, H.-L. Yip, S. K. Hau, and A. K.-Y. Jen, "Metal grid/conducting polymer hybrid transparent electrode for inverted polymer solar cells," Appl. Phys. Lett, vol. 96, no. 20, pp. 203301, May 2010.

[54] "http://www.2spi.com/catalog/standards/ITO-coated-slides-resistivities5.html."

[55] D. H. Shin, H. C. Shim, J.-W. Song, S. Kim, and C.-S. Han, "Conductivity of films made from single-walled carbon nanotubes in terms of bundle diameter," Scripta Mater, vol. 60, no. 8, pp. 607–610, Apr. 2009.

[56] L. Hu, G. Gruner, J. Gong, C.-J. "CJ" Kim, and B. Hornbostel, "Electrowetting devices with transparent single-walled carbon nanotube electrodes," Appl. Phys. Lett, vol. 90, no. 9, pp. 093124, 2007.

[57] S. De, P. J. King, P. E. Lyons, U. Khan, and J. N. Coleman, "Size Effects and the Problem with Percolation in Nanostructured Transparent Conductors," ACS Nano, vol. 4, no. 12, pp. 7064–7072, 2010.

[58] L. Yang, T. Zhang, H. Zhou, S. C. Price, B. J. Wiley, and W. You, "Solution-Processed Flexible Polymer Solar Cells with Silver Nanowire Electrodes," ACS Appl. Mater. Interfaces, vol. 3, no. 10, pp. 4075–4084, 2011.

[59] A. R. Madaria, A. Kumar, F. N. Ishikawa, and C. Zhou, "Uniform, highly conductive, and patterned transparent films of a percolating silver nanowire network on rigid and flexible substrates using a dry transfer technique," Nano Res, vol. 3, no. 8, pp. 564–573, 2010.

[60] C.-H. Liu and X. Yu, "Silver nanowire-based transparent, flexible, and conductive thin film," Nanoscale Res. Lett, vol. 6, no. 75, pp. 1–8, 2011.

[61] W. Gaynor, G. F. Burkhard, M. D. McGehee, and P. Peumans, "Smooth Nanowire/Polymer Composite Transparent Electrodes," Adv. Mat, vol. 23, no. 26, pp. 2905–2910, 2011.

[62] X.-Y. Zeng, Q.-K. Zhang, R.-M. Yu, and C.-Z. Lu, "A New Transparent Conductor: Silver Nanowire Film Buried at the Surface of a Transparent Polymer," Adv. Mat, vol. 22, no. 40, pp. 4484–4488, 2010.

[63] A. del Campo and C. Greiner, "SU-8: a photoresist for high-aspect-ratio and 3D submicron lithography," J. Micromech. Microeng, vol. 17, no. 6, p. R81, 2007.

[64] B. E. Hardin, W. Gaynor, I. Ding, S. B. Rim, P. Peumans, and M. D. McGehee, "Laminating solution-processed silver nanowire mesh electrodes onto solid-state dye-sensitized solar cells," Org. Elec, vol. 12, no. 6, pp. 875–879, 2011.

[65] Z. Yu, L. Li, Q. Zhang, W. Hu, and Q. Pei, "Silver Nanowire-Polymer Composite Electrodes for Efficient Polymer Solar Cells," Adv. Mat, vol. 23, no. 38, pp. 4453–4457, 2011.

[66] J. L. Elechiguerra, L. Larios-Lopez, C. Liu, D. Garcia-Gutierrez, A. Camacho-Bragado, and M. J. Yacaman, "Corrosion at the nanoscale: The case of silver nanowires and nanoparticles," Chem. Mat, vol. 17, no. 24, pp. 6042–6052, 2005.

[67] M. A. Green, K. Emery, Y. Hishikawa, W. Warta, and E. D. Dunlop, "Solar cell efficiency tables (version 39)," Progress in Photovoltaics: Research and Applications, vol. 20, no. 1, pp. 12–20, 2012.

[68]. The current density in the nanowires was estimated by dividing the total current flowing through the electrode by the total cross-sectional area of all nanowires contacting the copper strip at one end of the sample, and multiplying by two since we assumed only half the nanowires were involved in conduction.

[69] L. Hu, H. S. Kim, J. Y. Lee, P. Peumans, and Y. Cui, “Scalable coating and properties of transparent, flexible, silver nanowire electrodes,” ACS Nano, vol. 4, no. 5, pp. 2955–2963, 2010.

[70] X. Y. Zeng, Q. K. Zhang, R. M. Yu, and C. Z. Lu, “A new transparent conductor: silver nanowire film buried at the surface of a transparent polymer,” Adv. Mat vol. 22, no. 40, pp. 4484–4488, 2010.

[71] J. Krantz, M. Richter, S. Spallek, E. Spiecker, and C. J. Brabec, “Solution-Processed Metallic Nanowire Electrodes as Indium Tin Oxide Replacement for Thin-Film Solar Cells,” Adv. Func. Mat, 2011.

[72] H. R. Patil and H. B. Huntington, “Electromigration and associated void formation in silver,” J. Phys. Chem. Sol, vol. 31, no. 3, pp. 463–474, 1970.

[73] B. Stahlmecke, F. J. Meyer zu Heringdorf, L. I. Chelaru, M. Horn-von Hoegen, G. Dumpich, and K. R. Roos, “Electromigration in self-organized single-crystalline silver nanowires,” Appl. phys. Lett, vol. 88, no. 5, pp. 053122, 2006.

[74] Q. Huang, C. M. Lilley, and R. Divan, “An in situ investigation of electromigration in Cu nanowires,” Nanotechnology, vol. 20, no. 7, p. 075706, 2009.

[75] M. R. Kaspers, A. M. Bernhart, F. J. M. zu Heringdorf, G. Dumpich, and R. Möller, “Electromigration and potentiometry measurements of single-crystalline Ag nanowires under UHV conditions,” J. of Phys. Condensed Matter, vol. 21, no. 26, p. 265601, 2009.

[76] X. Liu, J. Zhu, C. Jin, L. M. Peng, D. Tang, and H. Cheng, “In situ electrical measurements of polytypic silver nanowires,” Nanotechnology, vol. 19, no. 8, p. 085711, 2008.

[77] J. L. Elechiguerra, L. Larios-Lopez, C. Liu, D. Garcia-Gutierrez, A. Camacho-Bragado, and M. J. Yacaman, "Corrosion at the nanoscale: The case of silver nanowires and nanoparticles," Chem. Mat, vol. 17, no. 24, pp. 6042–6052, 2005.

[78] J. P. Franey, G. W. Kammlott, and T. E. Graedel, "The corrosion of silver by atmospheric sulfurous gases," Corros. Sci, vol. 25, no. 2, pp. 133–143, 1985.

[79] Y. Sun, B. Mayers, T. Herricks, and Y. Xia, "Polyol synthesis of uniform silver nanowires: a plausible growth mechanism and the supporting evidence," Nano Lett, vol. 3, no. 7, pp. 955–960, 2003.

[80] Y. Sun, B. Mayers, and Y. Xia, "Transformation of Silver Nanospheres into Nanobelts and Triangular Nanoplates through a Thermal Process," Nano Lett, vol. 3, no. 5, pp. 675–679, 2003.

[81] M. E. Toimil Molares, A. G. Balogh, T. W. Cornelius, R. Neumann, and C. Trautmann, "Fragmentation of nanowires driven by Rayleigh instability," Appl. Phys. Lett, vol. 85, no. 22, p. 5337, 2004.

[82] N. Chawdhury, A. Köhler, M. G. Harrison, D. H. Hwang, A. B. Holmes, and R. H. Friend, "The effects of H_2O and O_2 on the photocurrent spectra of MEH-PPV," Syn. Met, vol. 102, no. 1, pp. 871–872, 1999.

[83] K. Kawano, R. Pacios, D. Poplavskyy, J. Nelson, D. D. C. Bradley, and J. R. Durrant, "Degradation of organic solar cells due to air exposure," Sol. Eng. Mat. Sol. Cel, vol. 90, no. 20, pp. 3520–3530, 2006.

[84] E. Voroshazi, B. Verreet, T. Aernouts, and P. Heremans, "Long-term operational lifetime and degradation analysis of P3HT: PCBM photovoltaic cells," Sol. Eng. Mat. Sol. Cel, vol. 95, no. 5, pp. 1303–1307, 2011.

[85] Y. Sun, C. J. Takacs, S. R. Cowan, J. H. Seo, X. Gong, A. Roy, and A. J. Heeger, "Efficient, Air-Stable Bulk Heterojunction Polymer Solar Cells Using MoOx as the Anode Interfacial Layer," Adv. Mat, vol. 23, no. 19, pp. 2226–2230, 2011.

[86] P. E. Burrows, V. Bulovic, S. R. Forrest, L. S. Sapochak, D. M. McCarty, and M. E. Thompson, "Reliability and degradation of organic light emitting devices," Appl. Phys. Lett, vol. 65, no. 23, pp. 2922–2924, 1994.

[87] G. Dennler, C. Lungenschmied, H. Neugebauer, N. S. Sariciftci, M. Latreche, G. Czeremuszkin, and M. R. Wertheimer, "A new encapsulation solution for flexible organic solar cells," Thin Solid Films, vol. 511, pp. 349–353, 2006.

[88] Y. Ahn, Y. Jeong, and Y. Lee, "Improved Thermal Oxidation Stability of Solution-Processable Silver Nanowire Transparent Electrode by Reduced Graphene Oxide," ACS Appl. Mater. Interfaces, vol. 4, no. 12, pp. 6410–6414, Dec. 2012.

[89] A. R. Rathmell, M. Nguyen, M. Chi, and B. J. Wiley, "Synthesis of oxidation-resistant cupronickel nanowires for transparent conducting nanowire networks," Nano Lett, vol. 12, no. 6, pp. 3193–3199, 2012.

[90] D. Kim, H.-C. Lee, J. Y. Woo, and C.-S. Han, "Thermal Behavior of Transparent Film Heaters Made of Single-Walled Carbon Nanotubes," J. Phys. Chem. C, vol. 114, no. 13, pp. 5817–5821, 2010.

[91] Y.-H. Yoon, J.-W. Song, D. Kim, J. Kim, J.-K. Park, S.-K. Oh, and C.-S. Han, "Transparent Film Heater Using Single-Walled Carbon Nanotubes," Adv. Mat, vol. 19, no. 23, pp. 4284–4287, 2007.

[92] J. Kang, H. Kim, K. S. Kim, S.-K. Lee, S. Bae, J.-H. Ahn, Y.-J. Kim, J.-B. Choi, and B. H. Hong, “High-Performance Graphene-Based Transparent Flexible Heaters,” Nano Lett, vol. 11, no. 12, pp. 5154–5158, 2011.

[93] D. Sui, Y. Huang, L. Huang, J. Liang, Y. Ma, and Y. Chen, “Flexible and Transparent Electrothermal Film Heaters Based on Graphene Materials,” Small, vol. 7, no. 22, pp. 3186–3192, 2011.

[94] E. Medvedovski, N. Alvarez, O. Yankov, and M. K. Olsson, “Advanced indium-tin oxide ceramics for sputtering targets,” Ceram. Inter, vol. 34, no. 5, pp. 1173–1182, 2008.

[95] “http://en.wikipedia.org/wiki/List_of_thermal_conductivities.” .

[96] C. Celle, C. Mayousse, E. Moreau, H. Basti, A. Carella, and J.-P. Simonato, “Highly flexible transparent film heaters based on random networks of silver nanowires,” Nano Res, vol. 5, no. 6, pp. 427–433, 2012.

[97] J. Morikawa and T. Hashimoto, “Study on thermal diffusivity of poly(ethylene terephthalate) and poly(ethylene naphthalate),” Polymer, vol. 38, no. 21, pp. 5397–5400, 1997.

[98] H. H. Khaligh and I. A. Goldthorpe, “Failure of silver nanowire transparent electrodes under current flow", Nanoscale Res. Lett, in press.